Assessing the relationship between hypoxia and life on Earth, and implications for the search for habitable exoplanets

Thomas Smith

Dissertations in Geology at Lund University,
Master's thesis, no 629
(45 hp/ECTS credits)

Department of Geology
Lund University
2022

Assessing the relationship between hypoxia and life on Earth, and implications for the search for habitable exoplanets

Master's thesis
Thomas Smith

Department of Geology
Lund University
2022

Contents

Cover Picture: https://www.universetoday.com/41702/picture-of-earth-from-space/

Assessing the relationship between hypoxia and life on Earth, and implications for the search for habitable exoplanets

THOMAS SMITH

Smith, T., 2022: Assessing the relationship between hypoxia and life on Earth, and implications for the search for habitable exoplanets. *Dissertations in Geology at Lund University*, No. 629, 44 pp. 45 hp (45 ECTS credits) .

Abstract: Atmospheric oxygen at the level of present-day Earth (21%) is generally regarded as permissive for the development and survival of complex multicellular life, such as animals. The hypothesis that oxic conditions are conducive for multicellular life has subsequently been applied to the search for life elsewhere in the universe, with planets exhibiting atmospheric oxygen of a similar level to Earth being considered as candidates for habitability. However, an opposing view states that in fact hypoxia (1–5% oxygen) is a prerequisite for tissue renewal, and therefore also for complex multicellularity. Hypoxia is present in many facets of life, such as during early mammalian embryogenesis as well as in niches like bone marrow, where populations of undifferentiated stem cells are maintained. This view implies that oxic conditions are indeed challenging for the evolution of complex multicellularity, and furthermore questions the association between oxic conditions and the potential for multicellular life on exoplanets.

Here, I review, test and discuss the association between hypoxic conditions and the evolution of complex multicellular life. Through an extensive study of the available literature, I review how hypoxia and cellular hypoxia-response machineries play a vital role in many stages of metazoan development, regulating the transcription of multiple genes and maintaining cell stemness during mammalian embryogenesis. I perform experiments to mimic the development of an hypoxic sedimentary niche on an exoplanet, and test how sediment grain size alters the depth of the hypoxic zone within these sediments. The results demonstrate that, in the absence of microorganisms, the hypoxic niche expands to greater depths within coarser sediments than in finer sediments. Where microorganisms were present within this sediment, the depth of the hypoxic niche was significantly reduced. Microbial respiration rapidly turned the sediment anoxic. Therefore, I propose that the absence of microorganisms within this type of sediment is advantageous for the maintenance and expansion of the hypoxic niche; however this absence may hinder the development of larger forms of life within these sediments.

I also evaluate the likelihood of hypoxic conditions on rocky exoplanets orbiting white dwarfs. Utilising data from extrasolar white dwarfs polluted by external material (that likely represents planets that formerly orbited the stars), oxygen fugacities are used as proxies for the oxidation state of these planetary atmospheres. These values are compared to oxygen fugacities of early and present-day Earth and Mars in order to observe the similarities between their atmospheric oxygen levels. It is concluded that one of the studied white dwarfs may have developed an hypoxic atmosphere during its lifetime, and thus that the former planet orbiting the star had the potential to hold complex multicellular life.

Keywords: hypoxia, hypoxia-inducible factors, atmospheric oxygen, multicellularity, embryogenesis, exoplanets, white dwarfs, oxygen fugacity

Supervisor(s): Sylvain Richoz, Emma Hammarlund

Subject: Biogeology

Thomas Smith, Department of Geology, Lund University, Sölvegatan 12, SE-223 62 Lund, Sweden. E-mail: thomas.smith772@gmail.com

Bedömning av förhållandet mellan hypoxi och livet på Jorden, samt dess konsekvenser för sökandet efter liv på andra planeter

THOMAS SMITH

Smith, T., 2022: Bedömning av förhållandet mellan hypoxi och livet på Jorden, samt dess konsekvenser för sökandet efter liv på andra planeter. *Examensarbeten i geologi vid Lunds universitet*, Nr. 629, 44 sid. 45 hp.

Sammanfattning: Atmosfärens höga syrekoncentration (nutid: 21%) anses allmänt ha varit nödvändigt för utvecklingen av komplexa flercelliga organismer, däribland djur. Därför har vi ofta utgått ifrån att syresatta förhållanden är nödvändiga för flercelligt liv även på andra platser i universum. Planeter som uppvisar syre i sin atmosfär anses således som goda kandidater för utvecklingen av flercelligt liv. En annan, direkt motsatt, hypotes anser dock att en låg syrehalt (hypoxiö 1-5% syre) i själva verket är en förutsättning för komplext flercelligt liv, eftersom det har visats vara avgörande för att vävnad ska kunna förnyas. Hypoxi är således vanligt förekommande i ett djurs livscykel, till exempel tidigt i embryogenesen hos däggdjur, samt kring odifferentierade stamceller i benmärgen som skall komma att ersätta gamla celler i kroppens vävnader. I och med att hypoxiska förhållanden är centrala för att utveckla och bibehålla komplex vävnad så kan syresatta förhållanden också anses försvårande för utvecklingen av komplex flercellighet, vilket i sin tur gör att vi kan ifrågasätta sambandet mellan oxiska förhållanden (hög syrehalt) och potentialen för flercelligt liv på exoplaneter.

I detta arbete granskar, testar och diskuterar jag sambandet mellan hypoxi och utvecklingen av komplext flercelligt liv. Genom en omfattande studie av tillgänglig litteratur granskas huruvida hypoxi samt cellulära mekanismer som styrs av hypoxi spelar en viktig roll i utvecklingsstadier av djur, samt hur hyopxi reglerar transkriptionen av gener och upprätthåller stamceller under däggdjurs embryogenes. Studien består även av experiment som strävar efter att efterlikna en hypoxisk sedimentär nisch på en exoplanet, för att testa hur sedimentens kornstorlek påverkar utbredningen av den hypoxiska zonen inom dessa sediment. Resultaten visar att den hyposiska nischen expanderar till ett större djup i grövre sediment än in finare sediment, i frånvaro av mikroorganismer. Med mikroorganismer närvarande i sedimenten minskade den hypoxiska nischens djup avsevärt, och mikrobiell syrekonsumtion gör att sedimenten blir övervägande syrefria. Därför föreslår jag att frånvaron av mikroorganismer inom denna typ av sediment är fördelaktigt för underhåll och expansion av den hypoxiska nischen, men att denna frånvaro kan hindra utvecklingen av större livsformer inom dessa sediment.

I denna rapport utvärderas också sannolikheten för hypoxiska förhållanden på steniga exoplaneter som kretsar kring vita dvärgar. Med data från vita dvärgar med föroreningar på sin yta (material som sannolikt representerar planeter som tidigare kretsade kring stjärnorna) används fritt syre som indikation på dessa planeters forna syrehalt i atmosfärerna. Dessa värden jämförs med fritt syre från tidigare och nuvarande atmosfärer på Jorden och Mars, för att diskutera likheter och skillnader mellan atmosfäriska syrenivåer på dessa planeter. Resultatet visar att en av de studerade vita dvärgarna kan ha utvecklat en hypoxisk atmosfär under sin livstid, vilket påsivar att den tidigare planeten som kretsade kring stjärnan haft potential att hysa den nisch där även komplext flercelligt liv kan utvecklas.

Nyckelord: hypoxi, hypoxi-inducerbara faktorer, atmosfäriskt syre, flercellularitet, embryogenes, exoplaneter, vita dvärgar, syreflykt

Handledare: Sylvain Richoz, Emma Hammarlund

Ämnesinriktning: Biogeologi

Thomas Smith, Geologiska institutionen, Lunds Universitet, Sölvegatan 12, 223 62 Lund, Sverige. E-post: thomas.smith772@gmail.com

1 Introduction

A certain level of free atmospheric oxygen (O_2) has long been thought of by the scientific community as a requirement for the development and survival of complex multicellular life (e.g., Nursall 1959; Knoll & Carroll 1999). Complex multicellularity refers to life which has developed a number of advanced techniques for survival within Earth's environments, including intercellular communication and tissue differentiation (Knoll 2011). Combining the abundance of complex multicellularity on the present Earth with the current O_2 concentration of the atmosphere (~21%), it is fairly logical to conclude that high oxygen levels facilitate the development of complex life. The majority of known multicellular life on Earth appears to rely heavily on O_2 as a key molecule for the provision of significant amounts of energy during aerobic cellular respiration (Schmidt-Rohr 2020), and oxygen is utilised in a number of chemical cycles and metabolic processes throughout the kingdoms of life (e.g., Halliwell & Gutteridge 2015). Whilst life is also known to have developed and persisted during the Proterozoic Eon (~2.5–0.54 Ga) and possibly as early as the Archaean Eon (~4.0–2.5 Ga) (Bell et al. 2015; Nutman et al. 2016), when O_2 concentrations were lower, it has often been assumed that the organisms during these periods remained small and uncomplex, at least compared to the vast complexity of life we see today (see fig 1 of Brocks & Banfield 2009).

An explosive radiation of animal life occurred across the Precambrian-Cambrian boundary and is often connected to a rise in atmospheric oxygen during the late-Neoproterozoic (see e.g., Bergman et al. 2004 and references therein). However, the view that the radiation of complex multicellularity awaited sufficient oxic conditions has been brought into question by subsequent discoveries of experimental multicellularity in the Paleoproterozoic (e.g., El Albani et al. 2010; Turner 2021), as well as oxygen levels 'sufficient' for the development of complex life in the Palaeo- and Mesoproterozoic (e.g., Bekker et al. 2004; Zhang et al 2016). This allows us to develop two connected hypotheses: that the Cambrian explosion was not necessarily a rapid expansion of the complexity of life on Earth, and that the complexity and size of life on Earth may not be so dependent on high atmospheric oxygen. If this is the case, alternative theories for the ideal oxygen conditions for the emergence of complex life must instead be explored. One hypothesis posits that hypoxia is required for the development of complex life (e.g., Hammarlund et al. 2018; Hammarlund 2020; Lee et al. 2020). If hypoxia, rather than high O_2, is indeed a requirement for the development of complex multicellularity, the way in which we observe the relationship between oxygen and life within scientific research will be dramatically altered, as we are forced to rethink our current understanding of the role of oxygen in multicellular life.

Hypoxia is context dependent, but refers in general to oxygen concentrations that are lower than 'normal' (atmospheric normoxia on Earth is currently ~21% oxygen). Hypoxia is encountered in many environments on Earth, both external environments (such as deep oceans and areas of high elevation) and within the tissues of many living organisms (including certain human tissues). Physiological hypoxia is defined as ~1–5% O_2 (Guzy & Schumacker 2006), whilst cellular hypoxia is ~0.2–5% O_2 (Lee et al. 2020).

The theory of high O_2 as a requirement for the development of complex multicellularity has also been expanded to the field of space research, specifically the search for habitable planets outside of our Solar System. Scientists frequently cite the presence of high atmospheric O_2 as a sign that an exoplanet has the potential to hold life (a biosignature, e.g., Meadows et al. 2018), and when regarding the evidence cited above, it is clear to see why this is the case. However, if the theory of hypoxia being required for life is true, this would expand the scope of exoplanet research: where previously only those exoplanets with similar levels of atmospheric oxygenation to our own have been considered as targets for potential habitability, this could potentially increase our chances of identifying habitable exoplanets.

This thesis explores the hypothesis that hypoxia is required for the development of complex multicellular life. An extensive literature review is undertaken to determine the role of hypoxia in the development of complex multicellularity as we understand it today. This review encompasses: the timelines of atmospheric oxygen and life on Earth; the possible oxygen requirements of early animals; the theorised link between high atmospheric O_2 and insect gigantism, and how this is in conflict with the hypoxia theory; the extent of hypoxic environments on present-day Earth; and the currently understood roles played by hypoxia in the development of life. This literature review will outline the argument that hypoxia, rather than high O_2, is required for the development of complex life. The rate of oxygen diffusion and the expansion of the hypoxic niche through different types of sediment will then be explored through experimental methods, the aim of which is to further narrow down the most conducive environment and conditions to search for life on other planets. This is then followed by an analytical estimation of the oxygen content of exoplanet atmospheres, in the hopes of expanding the search for habitable exoplanets to include those with reduced levels of atmospheric oxygen.

2 Background

Measurable oxygenation of the Earth's atmosphere can

be definitively traced back to the early Proterozoic, where an apparently rapid rise in atmospheric O_2 occurred (the GOE, 2.45–2.32 Ga, Bekker et al. 2004; Farquhar et al. 2014), followed later by the Neoproterozoic oxidation event (NOE, ~800–550 Ma; Canfield (2014)). Assuming there is a link between high atmospheric O_2 and the complexity of life, we should expect to see some kind of linear relationship between the oxygenation history of Earth's atmosphere and the development of complex life with a large increase in complexity following the GOE and the NOE. However, the relationship between oxygen and life, which will be explored in this section, may not be as linear as expected.

2.1 History of atmospheric oxygen

The link between oxygen and the development of life is difficult to constrain, not only due to the relative lack of appropriate proxies for atmospheric oxygenation the further back in time we go, but also due to the unreliability of the fossil record. The general scientific consensus, however, is that Earth's atmosphere during the Archaean (~4.0–2.5 Ga) was anoxic, $<10^{-5}$ PAL (present atmospheric levels) of O_2 (Bekker et al. 2004). Even after the GOE which began in the Late Archaean, atmospheric O_2 on Earth was still much lower than it is today. As can be seen in fig. 1, atmospheric O_2 was likely <10% PAL for much of the Proterozoic (Canfield 2014), meaning in actual terms there was ~2% oxygen in the atmosphere at this time (i.e., the atmosphere was hypoxic). It was not until the late Neoproterozoic–Phanerozoic that oxygen began to rise more towards present levels (Canfield 2014).

In addition to the values seen in fig. 1, many other authors have identified possible evidence for atmospheric oxygen levels at specific points in time. These include the estimate of 0.1–5% PAL at ~2.25 Ga (Yang & Holland 2003), >10% PAL but significantly lower than 100% PAL at ~2.0 Ga (Holland 2006), and ~4% PAL at ~1.4 Ga (Zhang et al. 2016). The huge variability of estimates for atmospheric oxygen levels throughout the Proterozoic outlines just how difficult it is to accurately determine atmospheric O_2 conditions this far back in time, however they generally support the hypothesis that Earth's atmosphere was hypoxic during the Proterozoic, even post-GOE.

2.2 History of life

The earliest forms of life likely emerged in the early-mid Archaean, with estimates ranging from 3.7 Ga (Ohmoto et al. 2014) to as far back at 4.1 Ga (Bell et al. 2015). These are of course difficult to prove, and much of the evidence is scarce and tells us nothing of the types of organisms that may have been present, merely the possible presence of biogenic material. It is reasonable to assume that the life at this time was very simple and anaerobic, due to the likelihood of an anoxic atmosphere during the Archaean.

Stromatolites are the earliest reported physical evidence for the presence of life is dated to ~3.7 Ga. Identified in the Isua Belt of Greenland by Nutman et al. (2016), these macroscale structures were interpreted as being of biogenic origin due partly to their resemblance of modern-day stromatolites. Stromatolites formed in recent-present times are commonly formed through the action of multiple types of microorganisms, such as sulphate-reducing bacteria and cyanobacteria which are the main carbonate producers (Dupraz et al. 2009; Riding 2011; Nutman et al. 2016). However, due to the anoxia of the Archaean atmosphere, it is likely that the earliest stromatolites were formed solely through the action of prokaryotic, filamentous bacteria (Astafieva 2019). It has also been proposed that early stromatolites show evidence of an autotrophic, carbon-fixing metabolism (Nutman et al. 2016). Regardless of how they were formed, these early stromatolites are an important indicator for the increasing complexity of life this early in Earth's history, providing evidence for life's ability to form complex communities capable of trapping sediment and building sedimentary structures.

Cyanobacteria are thought to be the first organisms to have practiced oxygenic photosynthesis on Earth, and therefore are frequently considered to have been heavily involved in the oxygenation of the Earth's atmosphere during the Proterozoic Era (e.g., Canfield 2005). This means that where we find the earliest evidence of oxygenic photosynthesis, we should find evidence of the earliest cyanobacteria, and vice versa. The earliest confirmed cyanobacteria exist from ~2.7–2.5 Ga, although molecular analysis suggests their origins began much earlier (Turner et al. 2001). Indeed, Rosing & Frei (2004) suggest that a negative $\delta^{13}C$ isotope signature from a pelagic shale of Greenland, when combined with its mode of occurrence, is indicative of highly productive planktonic organisms. This shale, although metamorphosed, is from >3.7 Ga, implying the possible presence of oxygenic photosynthesis and cyanobacteria this far back in time. However, as has been mentioned previously, the GOE did not begin until ~2.45 Ga, suggesting a number of possibilities: 1) that cyanobacteria did not evolve until their first confirmed appearance in the fossil record ~2.7–2.5 Ga; 2) that cyanobacteria were not the first organisms to practice oxygenic photosynthesis, and some other organisms were producing the signal identified by Rosing & Frei (2004); 3) that the earliest cyanobacteria evolved ~3.7 Ga, but did not initially practice oxygenic photosynthesis; or 4) the earliest cyanobacteria evolved ~3.7 Ga, and practiced oxygenic photosynthesis, but the oxygen produced was not sufficient to satisfy the various oxygen sinks of the Proterozoic Earth, so atmospheric oxygen did not rise

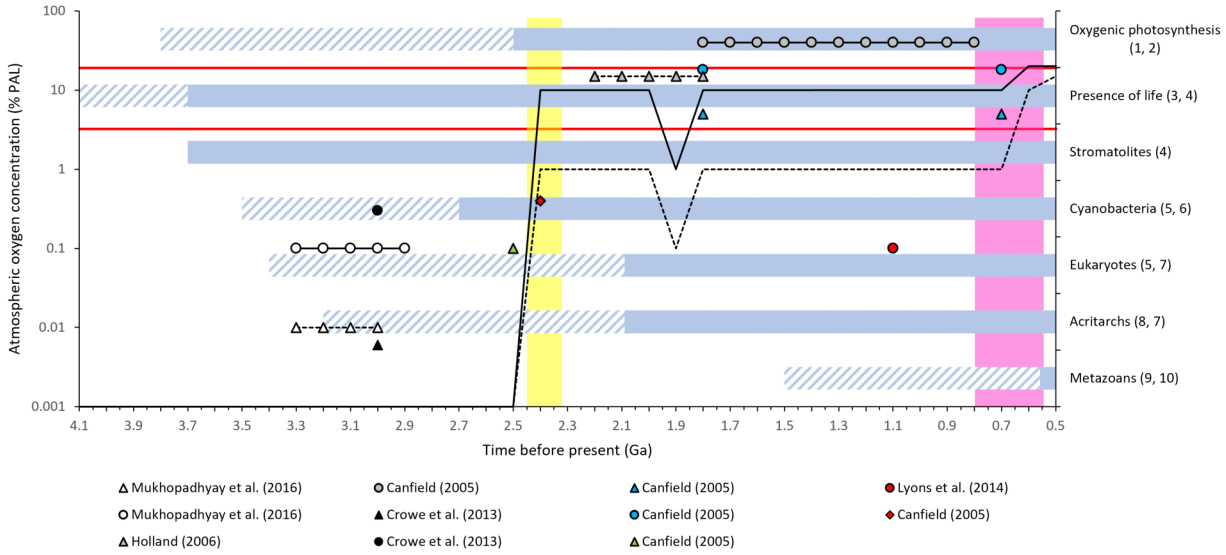

Fig. 1. a graph detailing the history of atmospheric oxygen on Earth from the Archaean to the early Phanerozoic, as well as the first emergence of certain types of life and oxygenic photosynthesis.

The solid and dashed black lines represent estimates for the maximum and minimum atmospheric oxygen levels of Earth respectively (Canfield 2014). The circles and triangles respectively represent other estimates for maximum and minimum atmospheric oxygen levels from a variety of sources, which are displayed in the legend above. The red diamond represents a possible maximum atmospheric oxygen level before 2.4 Ga (Canfield 2005). The striped blue bars represent the possible presence of certain organisms and oxygenic photosynthesis within the fossil record; the solid blue bars represent the definitive presence of these same groups. The numbers next to the labels of each group represent the following sources: 1) Buick (2008); 2) Hallman & Summons (2014); 3) Bell et al. (2015); 4) Nutman et al. (2016); 5) Astafieva (2019); 6) Canfield (2005); 7) Yin et al. (2020); 8) Buick (2010); 9) Robbins et al. (1985); 10) Bobrovskiy et al. (2018). The yellow column represents the Great Oxidation Event (GOE) from 2.45–2.32 Ga, based on the dates of Bekker et al. (2004). The pink column represents the Neoproterozoic oxidation event (NOE) from ~800–550 Ma according to Canfield (2014). The horizontal red lines represent rough estimates of the upper and lower limits of physiological hypoxia (1–5% oxygen, ~5–25% PAL).

until over one billion years later.

Eukaryotic multicellular organisms are consistently thought to require high levels of atmospheric oxygen in order to efficiently maintain metabolic and physiochemical functionality (e.g., Knoll & Carroll 1999; Semenza 2007). This would suggest that multicellular eukaryotes could not have evolved before the increase of atmospheric O_2 brought about by the GOE, or even possibly before the second increase of the NOE. The origin of eukaryotic multicellular life remains controversial and difficult to constrain, however many of the fossils proposed as evidence of eukaryotic forms places their evolution in the Palaeoproterozoic Era (some time before ~2.1–1.9 Ga, e.g., Han & Runnegar 1992; El Albani et al. 2010). The recent discovery of eukaryotic acritarchs from the Hutuo Group of China pushes back the evolution of eukaryotic metabolism to ~2.09–2.06 Ga (Yin et al. 2020), providing support for the presence of eukaryotes during this time. The eukaryotes discovered during this study are unicellular, and thus are not necessarily considered to require high oxygen for their survival, however this discovery may still be an indicator that eukaryotic evolution occurred during a period of lower atmospheric oxygen.

The origin of animals (metazoans) is equally as hard to determine as the origin of eukaryotes, with estimates ranging from the late Proterozoic to as far back as ~1.0 Ga. The earliest definitive evidence for metazoan activity is from ~0.558 Ga (558 Ma), in the form of lipid biomarkers produced by *Dickinsonia* (Bobrovskiy et al. 2018). It is likely that animals emerged before this time, with possible body fossils of early sponges existing from ~890 Ma (Turner 2021). The lack of evidence for metazoan life prior to the late Proterozoic may imply that the development of early animals was limited by the low oxygen conditions of the early-mid Proterozoic; however there is growing evidence to suggest that this would not have been the case.

After Holland (1984) proposed 10% PAL of O_2 as a minimum requirement for the emergence of the Cambrian fauna, subsequent authors have since concluded that the oxygen requirements of early animals were even lower than this. For example, Sperling et al. (2013) concluded that the bilaterian body plan would not have been prohibited unless O_2 was <0.4% PAL. Mills et al. (2014) expanded on this by studying modern demosponges, often considered an analogue for early animals. The studied demosponges were found to survive at oxygen concentrations of ~0.5–4% PAL. What is also of note from this study is that whilst exposure to low O_2 (~3–4% PAL) does not compromise the growth of the studied demosponges, the specimens

were still sensitive to anoxia (Mills et al. 2014). This reduced performance under anoxia is an indication that sponges (and by extension early metazoans) still required oxygen for their development, but that high levels of dissolved oxygen were not a necessity. This implies that early metazoans had the potential to develop under the reduced oxygen conditions of the Proterozoic Eon, and it also introduces the possibility that modern marine metazoans have retained this characteristic, and thus may be similarly capable of development under hypoxia, despite the apparent reliance of modern metazoans on increased oxygen concentrations.

Some previous mass extinctions have been attributed to oceanic anoxic events (e.g. Bartlett et al. 2018). This may appear to provide an argument against the hypothesis above, however as mentioned previously, Mills et al. (2014) found that whilst anoxic conditions were harmful to demosponges, hypoxic conditions were conducive for their development. This may suggest that these extinction events could have been caused by anoxia, as early metazoans would still have been affected by oxygen levels this low.

2.3 Insect gigantism and high oxygen

The observed increase in maximum insect body size of the Late Palaeozoic Era has frequently been linked to the apparent increase of atmospheric oxygen during this time to ~140–160% PAL (~30–35% of the atmosphere was oxygen, e.g., Harrison et al. 2010). This phenomenon has therefore often been presented as an example of the link between high atmospheric O_2 (hyperoxia) and the development of large complex life.

Whilst this apparent link appears to suggest that increased atmospheric oxygen is beneficial for the development of large multicellular life, there are a number of arguments against it. For example, Harrison et al. (2010) outline various arguments based on the potential inaccuracy of the fossil record in representing the Late Palaeozoic world, as well as examples of hyperoxia producing non-linear effects on body size within different insect species, suggesting that the influence of increased oxygen levels is not as simple as hyperoxia increasing insect body size. See Appendix A.1 for an in-depth discussion of these arguments. Whatever the case, the evidence for a link between hyperoxia and insect gigantism is far from conclusive, meaning it is unknown whether higher levels of atmospheric O_2 aids in the development of larger body plans for insects, and indeed any forms of multicellular life.

3 On the importance of low oxygen

3.1 The role of hypoxia in the development of life

Low oxygen (hypoxia) can be stated as essential for animal development (Lee et al. 2020). The maintenance of hypoxia within tissues has also been suggested essential to the radiation of animal life in Earth's oxic environments (e.g., Hammarlund et al. 2018; Hammarlund 2020). This idea will be explored in the following pages, focussing on examples of hypoxia being beneficial, and often required, for certain stages of life development. Studies involving human and animal embryonic stem cells will be highlighted, as well as studies of gene expression under hypoxia, and examples of responses to fluctuating oxygen conditions exhibited by several groups of organisms.

3.1.1 Hypoxia and embryogenesis

Most animals go through multiple phases of development during their life cycles; for example, mammals (including humans) develop from an embryo, and insects experience a larval development stage. These stages of development require different environmental conditions, including access to different levels of oxygen (e.g., Harrison et al 2010; Carroll et al. 2021). It is therefore reasonable to claim that consistently high O_2 levels are not optimal for all stages of the lifecycles of multicellular life. For instance, there is a large body of evidence for low oxygen conditions being required for the regular development of mammalian embryos. This relationship between oxygen levels and embryogenesis is strongly based on the oxygen sensitivity of stem cells.

Stem cells are difficult to fully encapsulate with one definition, but perhaps the best definition here is "a clonal, self-renewing entity that is multipotent and thus can generate several differentiated cell types" (Melton 2013, page 6). This essentially means that stem cells have the ability to remain 'undifferentiated' so they have the potential to become a variety of different cell types (pluripotency), depending on what kind of cell is required by the organism for tissue renewal. In addition to being constructed during development, most animal tissues also need to be renewed due to damage. This renewal occurs with stem cells. The maintenance of a stem cell population is therefore key for animals as it allows for the near-constant renewal of a large variety of cell types. This helps to maintain tissue function during times of stress, as well as potentially prolonging the life of the organism. Hypoxia on the order of <2% has been observed to maintain the undifferentiated state of stem cells, whereas exposure to higher oxygen levels (e.g., 21%) causes stem cells to differentiate (e.g., Ezashi et al. 2005).

Embryogenesis is associated with hypoxic conditions. The partial pressure of oxygen (pO_2) is known to be very low during the first stages of embryonic development. For example, human placental pO_2 levels are significantly lower than those of the surrounding protective tissue during the first 8–10 weeks of gestation (Rodesch et al. 1992). This is not exclusive to humans, as low oxygen conditions (specifically 5% O_2) are also essential during the first 24 hours of *in vitro* rat embryogenesis (Morriss & New 1979). During this first 24 hour period, the cranial neural fold is formed, which in mammalian development is critical for the development of the embryonic brain (Yamaguchi & Miura 2013). Embryos cultured under 20% O_2 for this first 24 hours exhibited a higher proportion of under-developed neural tubes (Morriss & New 1979). Although the neural tubes supported normal morphogenesis under 20% O_2 after the first 24 hours, this is already a significant indicator that hypoxia is required for some development stages of multiple forms of complex multicellular life.

Cellular machineries that are active at particularly hypoxic conditions have been studied since the 1990s, when transcription factors known as hypoxia-inducible factors (HIFs) were identified as being the most important proteins involved in the mammalian response to hypoxia (Semenza & Wang 1992). HIFs belong to a wide group of environmental sensors that regulate biological processes (Simon & Keith 2008); as the name suggests, HIFs specifically regulate the animal response to hypoxia. Multiple genes encode HIFs in different types of organisms, with the most common being HIF-1α expressed in most metazoans (Graham & Presnell 2017) and HIF-2α expressed only in vertebrates (Hammarlund et al. 2018). HIFs are seemingly restricted to animals, however molecules that appear to perform a similar function to HIFs have been identified in other groups of multicellular organisms, such as plants – these molecules will be explored in greater detail in Appendix A.2.

Mammalian development relies on HIFs. For example, it was found that when mice are deficient in HIF-1β, they exhibit vascular defects in multiple areas and subsequently express lethality by embryonic day 10.5 (Maltepe et al. 1997). A separate study published soon after found that mouse embryonic stem cells that were deficient in the subunit HIF-1α experienced multiple genetic and developmental defects, such as reduced levels of glycolytic enzyme-encoding mRNA, as well as neural tube and cardiovascular abnormalities (Iyer et al. 1998). This same study found that the embryos that developed these abnormalities experienced lethality by embryonic day 11 due to complete deficiency of HIF-1α. Both of these studies outline the importance of HIFs in the mammalian embryonic response to hypoxia. When combined with the essential nature of hypoxia during the initial stages of mammalian embryogenesis (e.g., Morriss & New 1979; Rodesch et al. 1992), HIF can be assumed to be also critical for the early development stages of other animals.

3.1.2 Gene expression

Oxygen is one of the most prominent physical abiotic pressures that influences the development and survival of life on Earth. Fluctuating oxygen levels therefore often influence gene expression within organisms, through the up- or down-regulation of genes involved in important processes such as protein transcription. This in turn controls the eventual physiological response of the organism to these fluctuating oxygen levels. These alterations in gene expression therefore constitute an important part of the hypoxic response of many organisms.

HIFs are known oxygen sensors, involved with a number of processes throughout the entire lifecycle of multicellular organisms. As the most prevalent controller of gene expression in response to hypoxia within animals, HIF-1α has a clear role in the control of gene expression in response to hypoxia. At the beginning of the 21st century, over twenty gene targets of HIF-1 had been identified, with multiple other genes also thought to be HIF-1α targets (Wenger 2002). A number of these genes are discussed in more detail in Appendix A.3; all that will be said here is that HIFs play a significant role in the up- or down-regulation of many metazoan genes in response to hypoxia.

A cell signalling pathway which promotes the undifferentiated state of stem cells during the metazoan hypoxic response has recently been identified in choanoflagellates (Richter et al. 2018). Within metazoans, this pathway is known to be a HIF target. HIFs are also thought to be exclusive to metazoans, making this discovery even more interesting. Choanoflagellates, which are protists, are the closest known evolutionary relatives to metazoans, suggesting that this signalling pathway, as well as HIFs and cellular control under hypoxia, may have evolved before the divergence of metazoans, and perhaps that the reliance of complex multicellularity on hypoxia is more ancient than the metazoa as well.

3.1.3 Responses to fluctuating oxygen

Many organisms on Earth are frequently exposed to fluctuations in oxygen, or live in hypoxic environments; such as oxygen minimum zones or at high altitudes. In what appear to be evolutionary responses to this exposure, various groups of multicellular organisms have developed a number of methods to maintain their metabolic functions within these conditions. However, it may be the case that these ‘adaptations’ were not developed to cope with conditions of de-

creased oxygenation, and that alternative explanations exist. This section will outline some of these observed responses to reduced oxygen conditions, such as metabolic depression techniques, a temporary switch to anaerobic respiration, and various physiological alterations. Possible alternative explanations for these responses will also be considered.

The most common behaviour exhibited by many organisms in response to hypoxia appears to be the reduction of metabolic rate (MR). This behaviour has been observed in a variety of organisms, including many groups of insects and other invertebrates (e.g., Guppy & Withers 1999; Harrison et al. 2006; Gorr et al. 2010). This behaviour is not exclusive to invertebrates (e.g., Boutilier et al. 1996), nor is it exclusive to the animal kingdom (e.g., Geigenberger et al. 2000). Many examples of this behaviour are outlined in Appendix A.4.

Organisms exposed to anoxic or hypoxic conditions often experience oxygen stress upon a return to conditions of increased oxygenation (reoxygenation). This can result in negative effects for the organism, such as the overproduction of reactive oxygen species (ROS), which can have various harmful effects for organisms (Hermes-Lima & Zenteno-Savin 2002; Halliwell & Gutteridge 2015). It is possible, however, for certain organisms to accommodate reoxygenation without experiencing this oxidative stress. For example, it was found that the goldenrod gall insects *Eurosta solidaginis* and *Epiblema scudderiana* did not suffer any damage during reoxygenation, apparently entirely due to the lowering of their metabolic rates (Joanisse & Storey 1998). This led these authors to conclude that the ability to enter a state of lowered metabolism was sufficient for these species to prevent damage caused by ROS upon reoxygenation. Reduction of MR may therefore be a method by which many organisms can survive fluctuating oxygen conditions within unstable environments

An additional response to hypoxia exhibited by many organisms is the switch to anaerobic respiration pathways. This is a fairly obvious response to a lack of atmospheric oxygen, and is somewhat linked to suppression of MR, as anaerobic respiration uses less energy-intensive chemical reactions to preserve the regular functions of the organism. A good example of this link between MR suppression and anaerobiosis is seen in the beetle species *Cicindela togata*, which suppresses its metabolism by 97% in response to anoxia (Hoback et al. 2000). This metabolic suppression appears to be further supported by anaerobic metabolic pathways, such as the utilisation of alternative metabolic substrates for the production of energy, and the subsequent conservation of ATP. This phenomenon is once again not exclusive to the animal kingdom, and more examples of the utilisation of anaerobic metabolic pathways and substrates by both plants and animals are available in Appendix A.5.

Organisms may also exhibit physiological changes in response to hypoxia including, for example, modifications to the tracheal respiratory systems of insects. Loudon (1989) reared larvae of the mealworm *Tenebrio molitor* in three different levels of ambient O_2 (21%, 15% and 10.5%), and found that the main tracheae had a greater cross-sectional area in lower ambient oxygen than those in normoxia. The main tracheae of larvae grown in 15% O_2 had a cross-sectional area 40% larger than larvae of the same size grown in 21% O_2. This tracheal area increase was even greater (120%) for those cultivated under 10.5% O_2 (Loudon 1989). This would seemingly allow the larvae to extract more O_2 from the oxygen-deprived air. Similar physiological alterations which result in the same outcome can be observed in other insect species. For example, it was found that at least one insect species, the blood-sucking bug *Rhodnius prolixus*, increased the number of tracheae within its body, rather than the cross-sectional area, as a result of being reared in reduced oxygen conditions (Harrison et al. 2006). Other ways in which insects alter their respiratory systems under hypoxia are outlined in Appendix A.6.

Insects can also display more general physiological variations as a response to altitude hypoxia. It has been found that insects can survive during these conditions, but the individuals found at these elevations display reduced wing size and flight capacity, along with a general reduction in body size (Hoback & Stanley 2001). This seemingly reduces the perceived oxygen requirements of these insects, thus allowing them to maintain high levels of metabolic activity under these reduced oxygen conditions. Whilst this does seem to place a size constraint on multicellular life under lower oxygen, it does still demonstrate that multicellular life is capable of maintaining metabolic function at very low levels of oxygen.

The majority of the examples outlined throughout this section appear to be responses/ adaptations to reduced oxygen conditions, implying that high atmospheric O_2 is indeed optimal for the development or survival of complex multicellular life. However, Hammarlund (2020) proposes an alternative theory. This author suggests that the silencing of HIFs under normoxia is an adaptation that has developed since the atmosphere became more oxygenated, and that the stabilisation of HIFs under hypoxia was actually the initial mode of function. This in turn implies that early multicellular organisms developed under (and were adapted to) low-oxygen conditions, and that HIF silencing was a later adaptation developed to assist organisms to better survive in an increasingly oxic world (Hammarlund 2020). Therefore, whilst the examples above appear to represent the responses of organisms to conditions of reduced oxygen, the utilisation of HIFs under hypoxia could instead signify the

initial mode of function of complex multicellular organisms. Perhaps complex multicellularity functions 'naturally' during hypoxia, with their HIFs activated, and they have gradually silenced their HIFs as the surface environments of Earth became more oxygenated. Hammarlund (2020) also proposes another theory: that a phenomenon observed within vertebrates may have made these organisms more dependent on high oxygen levels over time. This phenomenon, known as pseudohypoxia, makes vertebrates 'believe' they are living in an hypoxic environment, even when they are not, and it may have initially evolved as a way to combat the increasingly oxic environments of the Proterozoic world (Hammarlund 2020). This idea implies that it is less problematic for animals to live in environments with predictable oxygenation (stable) than when they fluctuate, in terms of stem cell maintenance and tissue renewal. HIF-1α would, however, allow animals to cope with fluctuations by for example mitigating the effects to switch the metabolic pathway. Even if the increase in oxygen did not imply HIF silencing or increased oxygen dependency of vertebrates, the paragraphs above still outline multiple examples of ways in which organisms are adapted to survive in reduced oxygen conditions, and therefore displays that complex multicellularity is still absolutely possible under hypoxia.

3.2 Hypoxic environments on the present Earth

Despite the high level of oxygenation of the present atmosphere, hypoxic environments are still prevalent on Earth. Some of these environments are naturally low in oxygen (e.g., Helly & Levin 2004; fig. 21.1 of Hourdez 2012), whilst others have become hypoxic or anoxic through anthropogenic influence (Diaz & Rosenberg 2008). A significant amount of biomass is also present within many of these hypoxic environments, indicating that low oxygen conditions are not necessarily a limiting factor for complex multicellular life.

Some of the most prominent hypoxic environments on Earth are oxygen minimum zones (OMZs) and areas of high elevation. OMZs are abundant in oceanic settings, especially in areas of nutrient upwelling along the western coasts of many landmasses, whilst hypoxia is well-known to affect organisms living in mountainous regions due to decreasing air pressure with increasing altitude (Hourdez 2012): at 5500 m above sea level, atmospheric O_2 reaches ~50% of that at sea level, decreasing even further to just 21% PAL at 12 000 m (Hourdez 2012). Additionally, the abundance of decaying organic matter on Earth (e.g., dead trees/large animals) constitutes another significant hypoxic niche. A low-oxygen environment which may not be thought of as frequently as those on the surface of the Earth is the deep subsurface. The subsurface of the Earth is known to be heavily populated, albeit mostly with bacteria and archaea (Bar-On et al. 2018). The extent of deep subsurface environments, as well as the extent of OMZs, and the biomass within both of these environments, is discussed at length in Appendix A.7. One interesting fact about the biota of the deep subsurface is the recent discovery of nematode species living within this harsh, low-oxygen environment (Danovaro et al. 2010). This discovery is an indicator that large forms of complex multicellular life are capable of survival (and currently exist) in environments of extremely low oxygen, suggesting that high levels of oxygen are not required for the survival of all complex multicellular organisms.

3.3 Future research

It is clear from the research outlined above that hypoxia plays a significant role in the development of complex multicellular life, and therefore this topic should be explored further in the future, especially if we wish to search for life on planets beyond our own. Of course, it will be difficult to fully understand the scope of the relationship between hypoxia and complex multicellularity due to the fact that most complex multicellular life today is adapted to the higher atmospheric oxygen that we experience on the present Earth, at least in the later stages of their development. Thus removing organisms from these conditions to study their response to hypoxia may not represent the true picture of the relationship between oxygen and life.

Future research within this field should focus on hypoxia inducible factors, and the genes which are targets for them. Through this research, it may be possible to identify more homologues for HIFs in more 'simple' organisms (prokaryotes, unicellular eukaryotes), enabling us to further understand how the relationship between hypoxia and complex multicellularity first came about, and possibly even when this relationship began.

Furthermore, through this research it may be possible to expand our search for extraterrestrial life. If we expand our understanding of modes of life other than those that rely on high atmospheric oxygen, we may stand a better chance of discovering planets with the potential to bear complex life in the near future. Experimental data will now be presented, with the hope of furthering research into the link between oxygen and life on Earth and other planets.

4 Experiments on the expansion of the sedimentary hypoxic niche

Upon attempting to research the extent and expansion of the hypoxic niche within different types of sediment

during this project, it became clear that this particular question is rarely addressed in the literature. Therefore, a simple experiment was designed in order to examine the diffusion of oxygen through different types of sediment. The aims of this experiment were twofold: firstly, to estimate the rate of O_2 consumption within different types of sediment under PAL of O_2, and how this rate is influenced by the presence or absence of microorganisms; and secondly, to estimate the influence of reduced atmospheric O_2 on the rate of O_2 diffusion through sediment, subsequently allowing for the determination of the size and rate of expansion of the hypoxic niche within these sediments. The details of this experiment will be outlined in the following section.

4.1 Methods for hypoxic niche experiment

4.1.1 Creating sediment samples

The sediments used for this experiment were a fine beach sand (grain size <100 μm) from the shores of Rännen, a lake in western-central Sweden (fig. 2), and JBL Sansibar dark, a fine granite sand designed for use in aquariums (grain size 200–600 μm). It is likely that the sand from Rännen is composed of glacial till due to the nature of the Quaternary deposits surrounding the lake (see fig. 2). These two types of sediment will be referred to as fine and coarse respectively.

For the first part of the experiment (determination of the rate of O_2 consumption), sediment samples were created by adding ~700 mL of each sediment to separate 1 L glass beakers, then adding deionised water and thoroughly mixing the samples until a total volume of ~900 mL was reached. These samples will be referred to as 'unclaved' hereafter, to contrast the autoclaved and double autoclaved samples to be described later. The top of each sediment sample was then pressed flat to create a uniform sediment surface (exchange surface area ~82 mm^2), and both samples were left to rest uncovered overnight. One sample of fine sediment was autoclaved in an attempt to remove the influence of microorganisms from the first part of the experiment. Autoclaving is a process which, through the use of high heat and pressure, is considered the only way to guarantee sterile conditions within glassware (Götz et al., 2014). The coarse sediment was not autoclaved as the oxygen measurements of the unclaved coarse sample seemed to suggest that microorganisms were already absent from the sediment (see fig. 3B and results/discussion).

To create the autoclaved fine sample, ~800 mL of fine sediment was poured into two 1 L-capacity glass bottles (~400 mL in each bottle), and each was covered with ~1 cm of deionised water. A slightly greater volume of sediment was autoclaved than was used to create the previous unclaved samples, in order to account for possible loss of sediment during both the autoclaving process and the final removal of the sediment from the bottles. The plastic lids of these bottles were loosely screwed on so the bottles did not break in the autoclave, and both bottles were then autoclaved for 20 minutes at 121°C. The bottles were removed from the autoclave once the pressure within the machine had reached zero, and the bottles were then allowed to cool completely with the lids screwed tightly on. Once cooled, the sediment from both bottles was transferred into one clean 1 L glass beaker, flushing the bottles with deionised water when required to remove as much sediment as possible. Deionised water was added to the beaker until a total volume of ~900 mL was reached, after which the new sample was mixed thoroughly and left to rest uncovered overnight.

For the second part of the experiment (determining the rate of O_2 diffusion through sediment under reduced atmospheric O_2), additional autoclaved samples were prepared using a similar method to above, but with some key differences, all of which were implemented in an attempt to reduce the presence and action of microorganisms as much as possible.

Firstly, both the fine and coarse sediments were autoclaved this time, as by this point the coarse sediment had been exposed to air for a significant amount of time, meaning microorganisms were likely now present in this sediment as well. This meant that 800 mL of both sediments were used, 400 mL in each glass bottle (using four bottles rather than two). Secondly, Milli-Q ultrapure water was used in the place of deionised water for all stages of the sample creation process (covering the sediment within the glass bottles before autoclaving, flushing the sediment out of the bottles and mixing with the sediment in the final samples). This Milli-Q water was used in place of deionised water in an attempt to remove the influence of microorganisms as much as possible, as it was thought that the use of deionised water may have been a factor in the introduction of microorganisms to the samples. Thirdly, the sediment to be used was autoclaved twice, and for 40 minutes each time rather than 20 minutes as with the previous autoclaved sample. All sediments were allowed to cool for 2–3 hours between each autoclaving session. Again, this was done in an attempt to remove the influence of microorganisms as much as possible, as it was observed during the first part of this experiment that autoclaving a single time may not have been sufficient to remove all microorganisms from the samples. The samples were then created using the same method as the previous autoclaved sample. Finally, the beakers containing the final samples were covered with Parafilm for as long as possible, with the samples only being uncovered when taking oxygen profiles or adjusting the oxygen concentra-

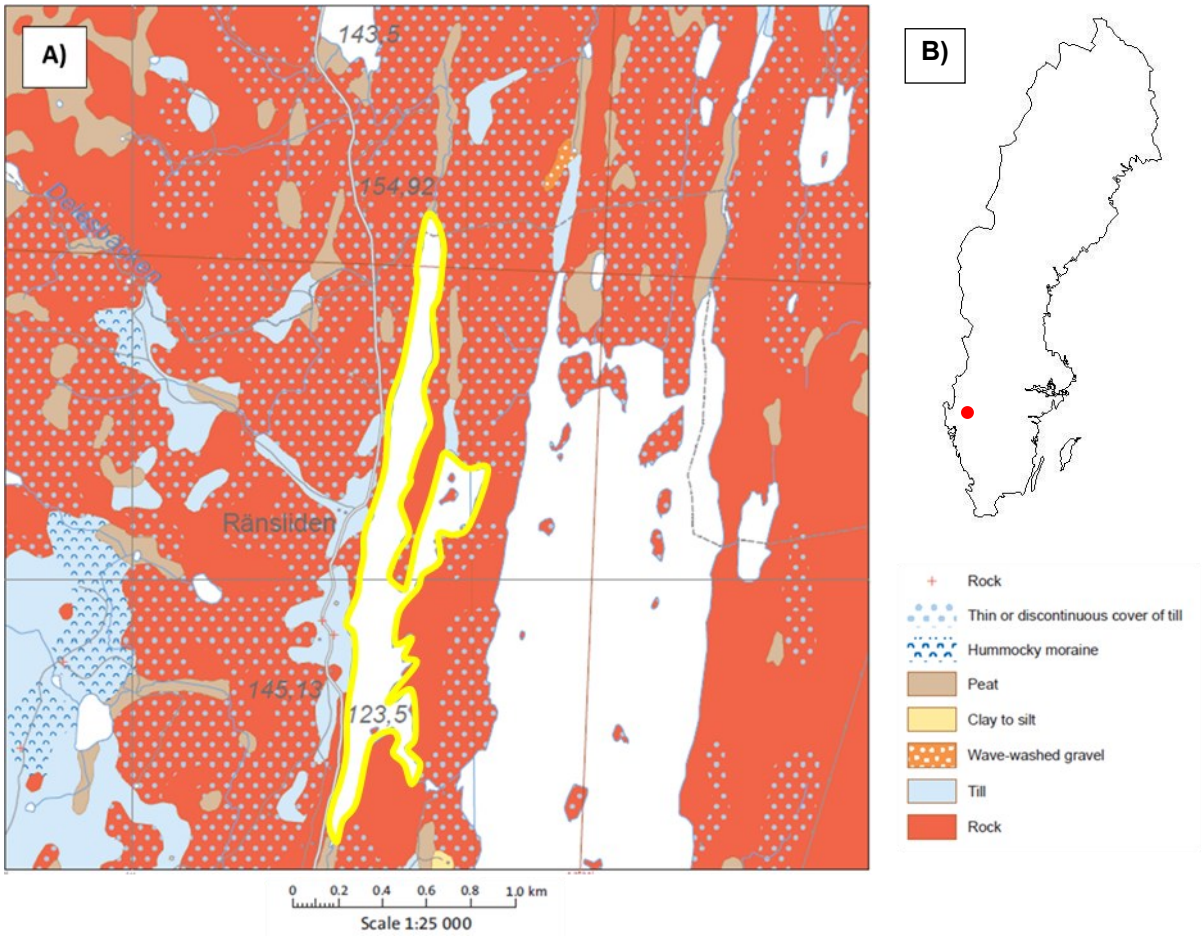

Fig. 2. a map showing Lake Rännen (**A**, highlighted in yellow) and the Quaternary deposits of the surrounding area. **B** shows the location of this lake in Sweden. Downloaded from the SGU map generator (http://apps.sgu.se/kartgenerator/maporder_en.html) on 01/06/2021.

tion, in an attempt to reduce contact with the ambient air.

4.1.2 Calibration of oxygen electrodes

A Unisense OX-500 oxygen micro electrode (outside tip diameter ~400–600 µm) was calibrated using the Unisense Profiling software. A calibration curve was created using two samples of deionised water: one 'untreated' sample (representing 21% oxygen, or 100% PAL), and one with the oxygen removed through treatment with sodium dithionite powder ($Na_2S_2O_4 + O_2 + H_2O$ à $NaHSO_4 + NaHSO_3$), representing 0% oxygen. The sensor was placed into the 0% oxygen water sample and was left until it reached a stable millivolt (mV) value, after which a measurement of the mV value was taken within the software and a point was created on the calibration curve. This process was then repeated with the 21% oxygen water sample, creating another point on the calibration curve. The curve created from these points was applied to the sensor and used in all future measurements with this sensor.

It should be noted that the measurements on the first two days for both unclaved sediment samples were taken using the Unisense OX-NP needle sensor for piercing (outside tip diameter 1.6 mm), with the curves produced being calibrated using this curve thereafter. The OX-NP sensor was unable to reach as deep into the sediment samples as the OX-500, and therefore the measurements taken on the first two days end at a much shallower level in the sediment than subsequent measurements. The only measurements affected by this included in this paper are the day 2 profiles of the fine and coarse unclaved samples.

4.1.3 Oxygen measurement

To measure the oxygen concentration within each sample, the calibrated Unisense OX-500 was suspended above the sample using the Unisense Micromanipulator, so that the tip of the sensor was ~1 cm below the surface of the overlying water. The Unisense SensorTrace Profiling software was then run to a total depth of -70 000 µm (-70 mm), with the sensor measuring the oxygen concentration in mV (uncalibrated) and micromoles per litre (µmol/L, calibrated) every 500 µm. This process was repeated at regular intervals of ~1–2 hours throughout each day, leaving the samples to rest in the closed laboratory between measure-

ments, uncovered for the unclaved and autoclaved samples, covered with Parafilm for the double-autoclaved samples.

When using the Unisense OX-NP on the unclaved samples for the first two days, the profiling software was only run to a total depth of -40 000 µm (-40 mm), with a measurement interval of 500 µm. The data obtained from all of the measurements was then exported from the Unisense SensorTrace Profiling software and Microsoft Excel was used to construct graphs to better display the data (figs. 3 and 4). In instances where two or more profiles obtained from the same sample on the same day had O_2 concentrations within ±10 µmol/L, a mean profile was calculated using the values of these profiles, and this mean profile was then used in the graph, as ±10 µmol/L was considered as a suitable margin of error for this experiment.

4.1.4 Oxygen control

For the second part of the experiment, the oxygen concentration of the water overlying the double-autoclaved samples was altered until it reached ~50% PAL (~10% oxygen). In order to facilitate better comparison between the profiles to be taken from these samples, 'control' profiles of the fine and coarse double-autoclaved samples were taken at 21% O_2 before the O_2 concentration was reduced. Small amounts of sodium dithionite powder were then mixed with the water overlying each sample, and the sediment and water of each sample were then mixed thoroughly. The oxygen concentration of the water overlying each sample was tested periodically using the Unisense OX-500 microsensor, with more sodium dithionite being added and the sample mixed again until the oxygen concentration of the water was ~0 µmol/L. A profile was then taken of the sample, in order to ensure that the oxygen concentration within the sediment was also at 0 µmol/L. If the sediment still had a higher oxygen concentration than the water, the process outlined above was repeated until the water and sediment showed the same concentration. This was done to ensure that any oxygen that may diffuse into the sediment during subsequent tests was from the air and overlying water, rather than it being trapped within the sediment itself.

Once the water and sediment had a uniform oxygen concentration, the overlying water was bubbled with 10% oxygen at a pressure of 0.5 atm, until the water reached an oxygen concentration equivalent to that of ~50% PAL (~10% in actual terms; in this case ~140 ± 10 µmol/L). At this point the samples were left to rest for ~1 hour covered with Parafilm. The samples were not mixed after the bubbling of 10% oxygen to ensure that any diffusion of oxygen into the sediment was a result of 'natural' diffusion and not due to physical disturbance. The oxygen concentration of the water overlying each sample was continuously tested throughout each day, with the concentration being maintained ~140 ± 10 µmol/L through bubbling of 10% O_2 and/or adding small amounts of sodium dithionite powder to the water. The sediment and water were also not mixed after these instances for the same reason as above.

4.1.5 Hypoxic niche calculation

In order to calculate the approximate vertical extent of the hypoxic niche for each profile, a line was drawn on each graph at 70 µmol/L, representing the approximate hypoxic threshold (5% atmospheric oxygen, black dashed line in figs. 3 and 4). The point on the y-axis (i.e. the depth) where each profile first crossed this line after entering the sediment was read from the graph, followed by the point at which the profile either reached anoxia or the point at which the profile crossed the hypoxic threshold again. The difference between these two values was calculated by subtracting the shallower depth from the greater depth. The resulting value represents the vertical extent of the hypoxic zone for each profile.

The traditional biological definition of anoxia (0 ml O_2/L) was used within this study, rather than the typical geological definition (0.2 ml/L). This is because the geological definition of anoxia is based on the supposed lower threshold of oxygen for protozoan and metazoan life – since this study concerns the relationship between low oxygen and life, I decided it was best to set the threshold of anoxia as the biological definition.

The vertical extent of the hypoxic niche was calculated for all samples, although it is mostly relevant to the samples used within the second part of the experiment.

4.2 Results of hypoxic niche experiment

A brief summary of the main trends observed within the results obtained through this experiment will be outlined here; more detailed descriptions can be found in Appendix B.1.

All the profiles obtained throughout this experiment show a similar trend, with the oxygen concentration decreasing with increasing sediment depth and increasing time. However, there are variations in the rate and extent of oxygen decrease between the profiles. This in turn means there are variations in the extent of the hypoxic zone between the profiles.

At 21% O_2, the oxygen content of the fine sediment (fig. 3A) remained constant the day after sample creation, followed by a slight decrease on day 3 then a much more significant decrease on day 4, with the oxygen content rapidly being depleted ~10 cm into the sediment. Autoclaving the fine sediment once did not appear to alter the results significantly (as seen in fig. 3C), with the oxygen being depleted at a similar sediment depth to the unclaved sample. However, double-

autoclaving the fine sediment seemed to cause the oxygen decrease to slow somewhat (fig. 4A), with the consequence of making the hypoxic zone slightly deeper than in the previous samples. A zone of hypoxia existed even nine days into the experiment, which was not true for the unclaved or single-autoclaved samples. It is important to note that for the double-autoclaved samples, the oxygen level was ~10% atmospheric O_2, not 21% as with the previous samples.

Within the coarse sediment, the unclaved sample measured at 21% O_2 did not reach hypoxia at all during the first four days of the experiment, with the profiles taken on days 3 and 4 showing remarkably similar oxygen levels (fig. 3B), in contrast to the fine sediment sample under the same conditions. The double-autoclaved coarse sample, however, showed a much more similar pattern to that of the fine double-autoclaved sample, with much slower decreases of oxygen content within the sediment and a much deeper hypoxic zone further into the experiment than with the unclaved sample (fig. 4B).

4.3 Discussion of hypoxic niche experiment

Throughout this experiment, the depth of hypoxia was measured in sediments of differing grain size and microbial content, as well as the impact of microbial content on the O_2 consumption rate. The results in general seem to suggest that the expansion of the hypoxic niche is greater within coarser sediment and in the absence of microorganisms, at least on these short timescales.

In terms of the impact of microbial content on O_2 consumption, there appears to be little difference between the consumption rate of O_2 within the unclaved and autoclaved fine sediment samples at 21% oxygen – in fact, the consumption was apparently faster in the autoclaved sample than in the unclaved sample, with the profiles reaching anoxia on day 4 of the unclaved sample and day 3 of the autoclaved sample. This could possibly mean that autoclaving the fine sediment a single time was not sufficient to remove all microorganisms from the sample. However, profile 2 of day 2 within the fine autoclaved sample had a much different pattern to that of either the day 2 or day 3 profiles of the unclaved sample: in the autoclaved sample, profile 2 of day 2 dipped briefly into hypoxia, before the O_2 concentration increased again back out of hypoxia by the end of the profile.

This is in contrast to the day 3 and day 4 profiles of the fine unclaved sediment, which showed patterns similar to those of day 2, profile 1 and day 3 of the fine autoclaved sample respectively. The dip into hypoxia exhibited by profile 2 of day 2 within the fine autoclaved sample may suggest that the autoclaving process was not sufficient to entirely remove the microorganism population from within the sediment, but that the population might have been reduced somewhat (i.e. microorganisms might still be present within the autoclaved sediment on day 2, but in smaller numbers, and were concentrated around the depth where the O_2 concentration began to decrease in profile 2, thus explaining the rapid decrease in O_2 concentration). This pattern is also present in the day 3 profile of the fine unclaved sample, with the O_2 concentration increasing deeper in the sediment, albeit much more slowly. This may suggest that the microorganisms within both the unclaved and autoclaved fine sediment samples were concentrated close to the sediment surface, and subsequently that autoclaving a single time was not sufficient to remove microorganisms from the sample.

The unclaved coarse sample does not reach hypoxia at all during the four days of the experiment, and the O_2 concentration within this sample remains much higher than that of either of the fine samples utilised for this part of the experiment. This sample was not autoclaved, which would ordinarily suggest the presence of microorganisms, however because the type of sediment utilised for this sample is commonly used as aquarium sand, it may have been devoid of microorganisms from the point of sample creation. This could explain the consistently high O_2 concentration within the sediment on the same timescale during which the oxygen disappeared from both fine samples.

It is also possible that the larger grain size of this sediment increased the porosity of the sample, allowing O_2 to diffuse more freely throughout the sediment. An interesting point for exploration in future experiments may be to run this experiment for longer, and measure the amount of time required for the development of hypoxia/anoxia within a unclaved sample of this coarser sediment. An additional idea may be to use coarse sand collected *in situ*, i.e. sand that had not been previously treated for use in aquariums, in order to observe how this alters the development of hypoxia.

The fine double-autoclaved sample used for the second part of the experiment exhibits an initial slight increase of the hypoxic niche followed by a significant decrease in the later days. The coarse double-autoclaved sample, however, shows the opposite pattern, with the hypoxic niche almost always increasing over subsequent days. Both of these samples were prepared in the same way, which suggests that the decreasing hypoxic niche of the fine double-autoclaved sample is not a function of the sediment being made anoxic, but rather that something to do with the sediment is decreasing the rate of O_2 diffusion. The fine sediment of course has a lower porosity than the coarse, as well as compacting more tightly, decreasing the diffusion potential of O_2 within the sediment.

The opposite relationship is also true – the increased grain size of the coarse sediment decreases the packing potential within the sample, increasing the

porosity and allowing O_2 to diffuse deeper into the sediment. This can be seen in fig. 4, which shows that not only does the hypoxic niche increase within this sample through time, but the depth at which the profiles reach anoxia increases as well. This implies that the hypoxic niche becomes deeper with time. Combining this with the theory of hypoxia being required for multicellular life might suggest that, beneath an atmosphere containing ~50% PAL of O_2, the sediment depth at which it is possible for multicellular life to develop increases for at least the first 2–8 days of exposure to this reduced-oxygen atmosphere. This experiment does not allow us to determine the expansion rate of the sedimentary hypoxic niche on geological timescales. Alternatively, it is possible that the double-autoclaving process was not sufficient to destroy all microorganisms within the sample, and the population subsequently recovered by day 5 to consume the oxygen more rapidly. This could be a possible consideration for future experiments – it may be worthwhile to autoclave the samples multiple times, or to utilise oth-

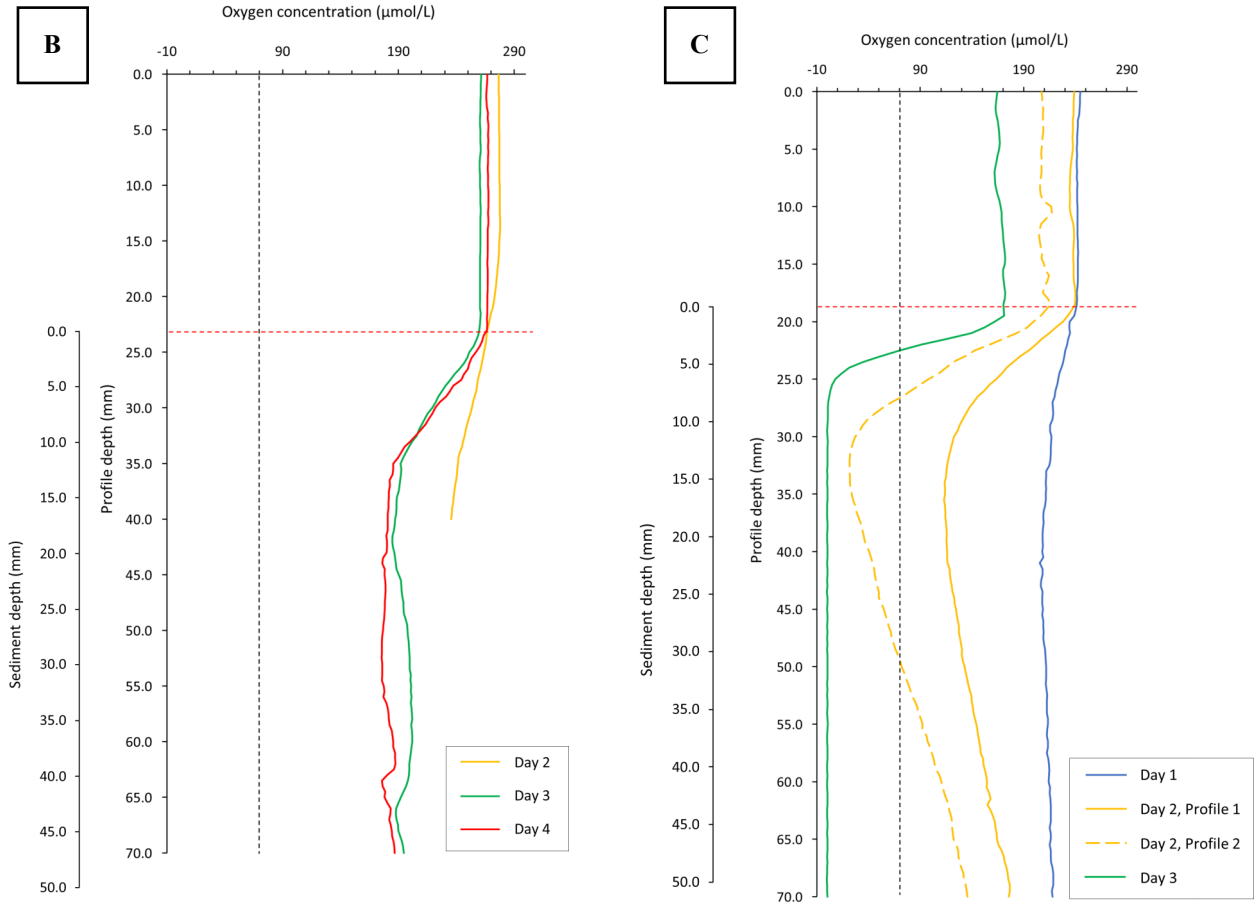

Fig. 3. graphs illustrating the results of the first part of the experiment outlined in the preceding pages. The dashed red line in each graph represents the sediment-water interface; the dashed black line represents the threshold for hypoxia. **A**) fine sediment, unclaved, 21% oxygen; **B**) coarse sediment, unclaved, 21% oxygen; **C**) fine sediment, autoclaved, 21% oxygen.

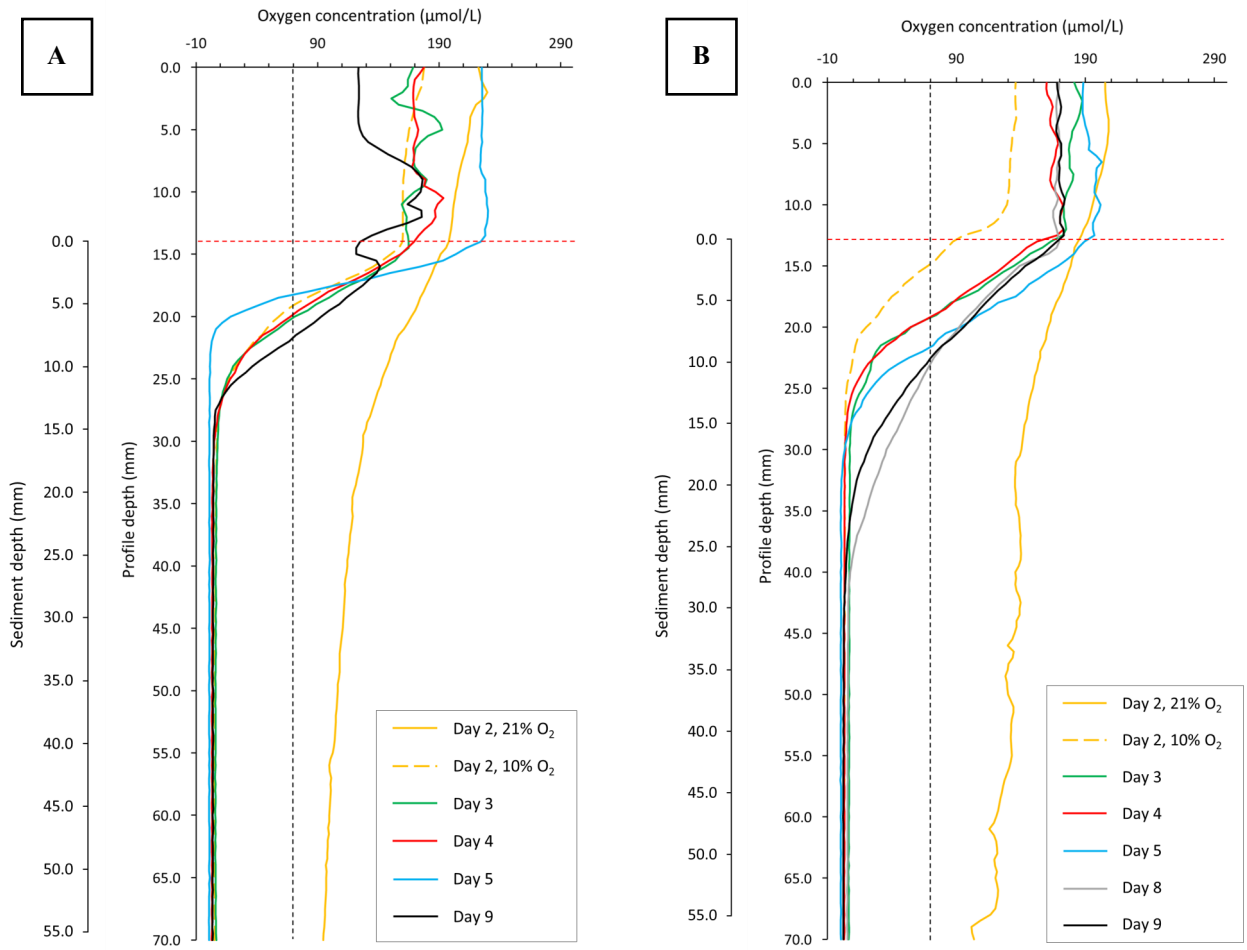

Fig. 4. graphs illustrating the results of the second part of the experiment outlined in the preceding pages. The dashed red line in each graph represents the sediment-water interface; the dashed black line represents the threshold for hypoxia. **A**) fine sediment, double autoclaved, 10% oxygen; **B**) coarse sediment, double autoclaved, 10% oxygen. The 'days' mentioned in correspond to the days after the sample was created (i.e. day 1 is the day of sample creation; day 2 is the day after sample creation etc.)

er methods to remove all possible microorganisms.

This experiment of course had many limitations, and there are many ways in which future experiments of this nature could be improved. For example neither part of this experiment considered the salinity of the water overlying each sediment sample, which would likely also be a factor influencing the diffusion potential of oxygen. Furthermore, consistently maintaining the oxygen concentration of the water overlying each sample was another considerable challenge within this experiment.

An interesting point for exploration in future experiments may be to run this experiment for longer, and measure the amount of time required for the development of hypoxia/anoxia within an unclaved sample of this coarser sediment. An additional idea may be to use coarse sand collected *in situ*, i.e. sand that had not been previously treated for use in aquariums, in order to observe how this alters the development of hypoxia. Finally, for the second part of the experiment, a control profile could be taken at the beginning of each day, rather than just the beginning of the experiment, as this would allow for more precise comparisons between the profiles taken at reduced oxygen on each day.

In conclusion, this experiment has expanded our knowledge of the behaviour of oxygen within aquatic sediments, in relation to the concentration of atmospheric oxygen, as well as the type of sediment through which the oxygen is travelling, and the influence of microorganisms on this transport. The hypoxic niche seems to expand to greater depths within coarser sediment than finer sediment under the absence of microorganisms, at least on the timescales of this experiment. This appears to be counterintuitive to the argument that hypoxia is beneficial/required for the development of larger life, as the presence of microorganisms would presumably be beneficial for the development of larger life, due to the production of nutrients through their metabolic processes and their eventual decay, as well as their influence on the environ-

mental conditions within the sediment itself (e.g., changing the pH of the sediment).

However, any microorganisms present would likely have consumed the oxygen within this hypoxic niche, rapidly producing anoxia and reducing both the size of the hypoxic niche and the chances of larger life developing. On the other hand, the hypoxic niche was found to be relatively small even in the absence of microorganisms, perhaps suggesting that the potential for complex life to develop under these conditions is limited regardless of the presence or absence of microorganisms. However, this experiment was done on a very small scale, and there is ample room for improvement, thus the potential for the expansion of the hypoxic niche and the development of complex life may be considerably different on larger or longer timescales.

5 Exoplanet oxygen

5.1 Background

As has been thoroughly discussed throughout this paper, a certain level of atmospheric oxygen is thought of as a requirement for the development and persistence of large multicellular life. This is based partially on the fact that Earth is currently the only example a planet that definitively holds life. This led to atmospheric oxygen being considered as an important biosignature in the field of space research, i.e. a sign that a planet may hold life (Meadows et al. 2018). It is very difficult to directly measure the contents of exoplanet atmospheres, due primarily to the vast distances between solar systems making it presently impossible to send physical objects from Earth to other stars. This means we must rely on more indirect methods for determining the geochemical composition of exoplanet atmospheres; one of these methods being analysing the chemical composition of polluted white dwarf (WD) atmospheres.

White dwarfs are the small, dense final stages in the life cycle of many stars (Doyle et al. 2019a), which are often observed to be 'polluted' by external material. It is likely that this polluting material originates from rocky bodies (i.e. planets or asteroids) that previously orbited the star (e.g., Gänsicke et al. 2012). By analysing the chemical composition of the atmospheres of these polluted WDs, it is thus possible to determine the geochemical characteristics of the bodies that orbited them. Doyle et al. (2019a) applied this theory to six polluted WDs in order to determine the oxygen fugacity of the parent bodies that polluted them, and subsequently compared these results to those for rocky planets in our Solar System, including Earth, to determine their geochemical similarity. Oxygen fugacity (fO_2) measures the degree of oxidation of a material – in the case of Doyle et al. (2019a) as well as this paper, this material is the rocks that make up a planet or planetary body. This means that fO_2 represents the "effective partial pressure of gaseous oxygen that would be in thermodynamic equilibrium with the material of interest" (Doyle et al. 2019a, page 1), and fO_2 is therefore a factor in the determination of many of the initial properties of a planet, including the composition of its atmosphere (e.g., Wetzel et al. 2013). Oxygen fugacity can thus be thought of as a proxy for atmospheric oxygen concentration, and fO_2 data from polluted WDs can be used to approximate the atmospheric oxygen concentration of the exoplanets that previously orbited these stars. This will subsequently allow us to search for planets with 'appropriate' atmospheric oxygen concentrations for the development of life. Ordinarily, scientists searching for oxygen as a biosignature would hope to find exoplanets with atmospheric concentrations similar to our own, however in the case of this paper, this method will instead be utilised in an attempt to locate exoplanets with lower concentrations of atmospheric oxygen.

5.2 Method for exoplanet calculations

Here, the analytical method outlined in Doyle et al. (2019c) will be used to calculate the fO_2 values of multiple polluted WDs. The elemental abundance data for the polluted WDs used in this paper (listed in table 1) were obtained from Harrison et al. (2018), Doyle et al. (2019b) and Doyle (2021); the majority of the data from these papers has been obtained from other sources, which are also outlined in table 1. The oxygen fugacities of Bulk Silicate Earth (BSE) and Bulk Silicate Mars (BSM) are also presented within this study for the sake of comparison, as was the case in Doyle et al. (2019a). BSE and BSM are used as references because they represent the 'primitive mantles' of Earth and Mars, after the formation of their iron-rich cores but before crustal differentiation (Pinti 2014). The geochemical compositions of these primitive bodies were similar to those of the polluted WDs used for this study, therefore allowing for more accurate comparison of the calculated fO_2 values.

The fO_2 values, the data used to calculate these values, and all associated errors for BSE and BSM have been taken directly from the Doyle et al. (2019b), with the original works this data was derived from also cited in table 1 and referenced at the end of this paper. The fO_2 values and the associated errors for the polluted WDs used in this paper (see table 2) have been calculated using the method explained in Appendix B.2, which is taken from Doyle et al. (2019c). When applying the method of Doyle et al. (2019c), it became apparent that the fO_2 values and the associated positive and negative errors for two of the WDs (WD 1145+017 and WD 1226+110) had been 'swapped' with each other within Doyle et al. (2019b) (i.e. the

data for WD 1145+017 produced the fO_2 and errors for WD 1226+110, and vice versa). It was assumed that this was a formatting error within Doyle et al. (2019b), and therefore the results for these two WDs presented in this paper have been 'swapped' back to what the appropriate values appear to be.

Doyle et al. (2019a) calculated the intrinsic oxygen fugacities of planetary bodies that previously orbited white dwarfs, i.e. the fO_2 at the time of formation of these planetary bodies. The basic methodology of these authors was to 'assign' oxygen to various metal species (Si, Mg, Al, Ca and Fe) identified in the atmospheres of polluted WDs, in order to form metal oxides; the metal oxides formed from this assignment represent the major minerals that make up the rocks of the polluting bodies which formerly orbited the star. By assigning oxygen to these metals in the order listed above, the amount of oxidised iron within the body could be calculated, allowing for the calculation of fO_2; any excess Fe not bonded to oxygen must have existed as metal, and was therefore assigned to the core of the body (Doyle et al. 2019a). The method used for this calculation is outlined in Appendix B.2. Polluted WD data was chosen primarily due to the knowledge that the polluting parent bodies were rocky, making for more accurate comparison to Earth and Mars (Doyle et al. 2019a). The calculated fO_2 values are presented relative to the Iron-Wüstite (IW) reference standard, Fe (Iron) + ½ O_2 = FeO (Wüstite), (Doyle et al. 2019a). The unit for fO_2 within this study is therefore ΔIW (change in IW, i.e. how different the fO_2 values are from the IW standard value). This comparison is common for rocky planets, as it reduces the influence of physical parameters (e.g., temperature and pressure) on the values obtained for fO_2 (Doyle et al. 2019a). The conversion of iron to wüstite in the reaction above has a specific, known oxygen fugacity at a variety of specific temperatures. Therefore if the temperature is a known quantity, then we also know what the fO_2 value 'should' be. The calculated fO_2 can then be compared to this reference value, with the difference between the values effectively removing the influence of physical parameters from the equation. In the case of Doyle et al. (2019a) and this present study, the temperatures of the WDs are known, meaning the calculated fO_2 values are relative to IW.

Oxygen fugacity is often measured compared to different standards, depending on how oxidising or reducing the material is – for example, the IW standard is commonly used for materials that are more reducing, whereas the quartz-fayalite-magnetite (QFM) standard is used for materials that are more oxidising. The present-day upper mantles of Earth and Mars are relatively oxidising, and thus the fO_2 values for these materials are most often presented relative to the QFM standard: the upper mantle of Earth has an approximate fO_2 of QFM ±2 log units (Frost & McCammon 2008), whilst that of Mars is QFM ±3 log units (Herd et al. 2002).

Polluted WDs with helium-dominated atmospheres were primarily chosen for this study, rather than those dominated by hydrogen, due to the disparity between the metal settling times of these two white dwarf varieties. The settling time of an element refers to how long it takes for the element to diffuse through the atmosphere of a white dwarf – H-dominated WDs have very short settling times, whereas those for He-dominated WDs are much longer (Montgomery et al. 2008). This shorter settling time makes it likely that any H-dominated WD with a polluted atmosphere is actively accreting material, and therefore that the material being accreted is not evenly distributed across the surface of the star (Montgomery et al. 2008). The elemental abundance data of H-dominated WD atmospheres must be corrected for this, whereas the same is not required for data from He-dominated WDs due to their much longer settling times. Doyle et al. (2019a) corrected for these settling times by calculating the area-integrated flux for the two H-dominated WDs within their study (available in table 1), and as a result the only H-dominated WDs included within this study are those from Doyle et al. (2019b).

The fO_2 values for the polluted WDs within this study were calculated using the equations outlined in Appendix B.2, taken from Doyle et al. (2019c). The data used to calculate these values is available in table 1.

5.3 Results of exoplanet calculations

The polluted WDs present within this study show a wide range of fO_2 values (see fig. 5 and table 2). The results will be very briefly outlined here; for a more in-depth look at the results, see Appendix B.3, where the WDs are grouped according to the papers from which their data was sourced for this study, not the original papers in which the data was published.

As can be seen from fig. 5, the majority of the WDs within this study show oxygen fugacity values within the range estimated for BSE and BSM, with some showing slightly more oxidising values and two being slightly more reducing. There appears to be no correlation between the type of atmosphere exhibited by the WD (H or He-dominated) and the oxygen fugacity of the star. The WDs with more reducing values generally appear to have greater uncertainty ranges than those that are more oxidising. Interestingly, the most reducing WDs do not have negative (i.e. more reducing) uncertainty ranges, only ones that are positive (more oxidising).

5.4 Discussion of exoplanet calculations

The fO_2 values of BSE and BSM are highly reducing (more negative fO_2 values are more reducing, and more positive values are more oxidising). The present-day upper mantle of Earth, on the other hand, has a relatively higher fO_2 (as seen in fig. 5), and thus is more oxidising. This difference between BSE and the present-day mantle can also be seen simply by observing the standards to which the fO_2 values for the two materials are compared, as was mentioned above: the IW standard to which the BSE, BSM and all polluted WDs in this study are compared is used to measure more reducing sources, whilst the present-day upper mantle is compared to the QFM standard, which is used for more oxidising materials. The approximate relationship between these two standards is as follows: $\Delta IW = \Delta QFM - 4$ (Doyle et al. 2019a).

The exact mechanisms by which the mantle became oxidising are still debated, and will only be touched upon briefly here. One possible theory involves plate tectonics, with convection slowly increasing the oxidation state of the mantle through the recycling of volatiles, whilst another suggests a role for the escape of gases such as hydrogen from the early atmosphere (e.g., Kasting et al. 1993). These possibilities will be further considered below, in regard to the limitations of this study; however, of more immediate interest to this study is the timeline of mantle oxidation, as this may relate to the relationship between the fO_2 of the mantle and the oxygen concentration of Earth's atmosphere. This relationship may then be extrapolated to exoplanets in the search for habitable extraterrestrial environments.

There are conflicting theories regarding the changing oxidation state of the Earth's mantle, with some authors suggesting that it has remained within ±2 log units of QFM (i.e. oxidising) since at least the Archaean (e.g., Schaefer & Fegley 2017), and others suggesting it became more oxidising around the Archaean -Proterozoic boundary, closer to the GOE. For example, Wang et al. (2020) theorise that the oxidation state of the mantle has influenced the atmospheric oxygen concentration through time, linking oxygenation events to major periods of supercontinental breakup. These authors thus conclude that the mantle became more oxidised around the Archaean-Proterozoic boundary, and subsequent volcanism and degassing from the oxidising upper mantle throughout history (as

Table 1. a list of the white dwarf (WD) stars used in this study, outlining the temperature of these stars and the elemental abundance data used to calculate their oxygen fugacities, as well as the errors associated with this data. **A**) WDs with helium-dominated atmospheres; **B**) WDs with hydrogen-dominated atmospheres; **C**) the objects used as reference materials within this study. The papers from which the data was sourced are listed in the rightmost column. The elemental abundances and associated errors for tables 1**A** and 1**C** are in log(Z/X), with Z being the element in question and X being either hydrogen (H) or helium (He), depending on the type of star. The data of table 1**B** has been corrected for settling times by Doyle et al. (2019a), and therefore has units of log(Z mol/s). This data can be treated as log(Z/X) values in the following equations. The associated errors for the data in tables 1**A**–**C** are represented throughout this paper by σlog(Z/X).

A

Object	Temperature (K)	O	Si	Mg	Al	Ca	Fe	Reference
WD 1145+017	16 900	-4.3 ± 0.5	-5.69 ± 0.09	-5.49 ± 0.1	-6.74 ± 0.1	-6.57 ± 0.1	-5.35 ± 0.1	Xu et al. (2016)
WD 1536+520	20 800	-3.4 ± 0.15	-4.32 ± 0.15	-4.06 ± 0.15	-5.38 ± 0.15	-5.28 ± 0.15	-4.5 ± 0.15	Farihi et al. (2016)
GD 40	15 300	-5.62 ± 0.1	-6.44 ± 0.3	-6.2 ± 0.16	-7.35 ± 0.12	-6.9 ± 0.2	-6.47 ± 0.12	Jura et al. (2012)
J0738+1835	13 950	-3.81 ± 0.19	-4.9 ± 0.16	-4.68 ± 0.07	-6.39 ± 0.11	-6.23 ± 0.15	-4.98 ± 0.09	Dufour et al. (2012)
GD 362	10 500	-5.14	-5.84 ± 0.3	-5.98 ± 0.25	-6.4 ± 0.2	-6.24 ± 0.1	-5.65 ± 0.1	Xu et al. (2013)
PG 1225-079	10 800	-5.54	-7.45 ± 0.1	-7.5 ± 0.2	-7.84	-8.06 ± 0.03	-7.42 ± 0.07	Xu et al. (2013)
J1242+5226	13 000	-4.3 ± 0.1	-5.3 ± 0.06	-5.26 ± 0.15	-6.5	-6.53 ± 0.1	-5.9 ± 0.15	Raddi et al. (2015)
HS 2253+8023	14 400	-5.37 ± 0.07	-6.27 ± 0.03	-6.1 ± 0.04	-6.7	-6.99 ± 0.03	-6.17 ± 0.03	Klein et al. (2011)
G241-6	15 300	-5.64 ± 0.11	-6.62 ± 0.2	-6.26 ± 0.1	-7.7	-7.3 ± 0.2	-6.82 ± 0.14	Jura et al. (2012)
GD 61	17 300	-5.93 ± 0.2	-6.83 ± 0.08	-6.63 ± 0.18	-7.18	-7.88 ± 0.19	-7.73 ± 0.2	Farihi et al. (2011)
J0845+2257	19 780	-4.25 ± 0.2	-4.8 ± 0.3	-4.7 ± 0.15	-5.7 ± 0.15	-5.95 ± 0.1	-4.6 ± 0.2	Wilson et al. (2015)
GALEX J2339	13 735	-5.52 ± 0.045	-6.59 ± 0.075	-6.58 ± 0.125	-7.7	-8.03 ± 0.505	-6.99 ± 0.24	Klein et al. (2021)
GD 378	15 620	-6.04 ± 0.245	-7.49 ± 0.105	-7.44 ± 0.17	-7.7	-8.7 ± 0.51	-7.51 ± 0.275	Klein et al. (2021)
WD 0446-255	10 120	-5.8 ± 0.1	-6.5 ± 0.1	-6.6 ± 0.1	-7.3 ± 0.3	-7.4 ± 0.1	-6.9 ± 0.1	Swan et al. (2019)
WD 1232+563	11 787	-5.14 ± 0.15	-6.36 ± 0.13	-6.09 ± 0.05	-7.5	-7.69 ± 0.05	-6.45 ± 0.11	Xu et al. (2019)
WD 2207+121	14 752	-5.32 ± 0.15	-6.17 ± 0.11	-6.15 ± 0.1	-7.08 ± 0.15	-7.4 ± 0.08	-6.46 ± 0.13	Xu et al. (2019)
WD 1551+175	14 756	-5.48 ± 0.15	-6.33 ± 0.1	-6.29 ± 0.05	-6.99 ± 0.15	-6.93 ± 0.07	-6.6 ± 0.1	Xu et al. (2019)

B

Object	Temperature (K)	O	Si	Mg	Al	Ca	Mg	Reference
WD1226+110	20 900	7.227 ± 0.2	6.233 ± 0.2	6.121 ± 0.2	5.641 ± 0.2	5.593 ± 0.2	6.489 ± 0.3	Doyle et al. (2019) Data S1
J1043+0855	18 330	6.52 ± 0.2	5.913 ± 0.5	5.995 ± 0.2	4.113 ± 0.3	5.351 ± 0.2	5.367 ± 0.3	Doyle et al. (2019) Data S1

C

Object	Temperature (K)	O	Si	Mg	Al	Ca	Fe	Reference
Bulk silicate Earth	N/A	-5.884 ± 0.1	-6.45 ± 0.3	-6.351 ± 0.16	-7.384 ± 0.12	-7.524 ± 0.2	-7.274 ± 0.12	Doyle et al. (2019) Data S1; McDonough (2003)
Bulk silicate Mars	N/A	-5.905 ± 0.1	-6.45 ± 0.3	-6.433 ± 0.16	-7.837 ± 0.12	-7.675 ± 0.2	-6.911 ± 0.12	Doyle et al. (2019) Data S1; Taylor (2013)

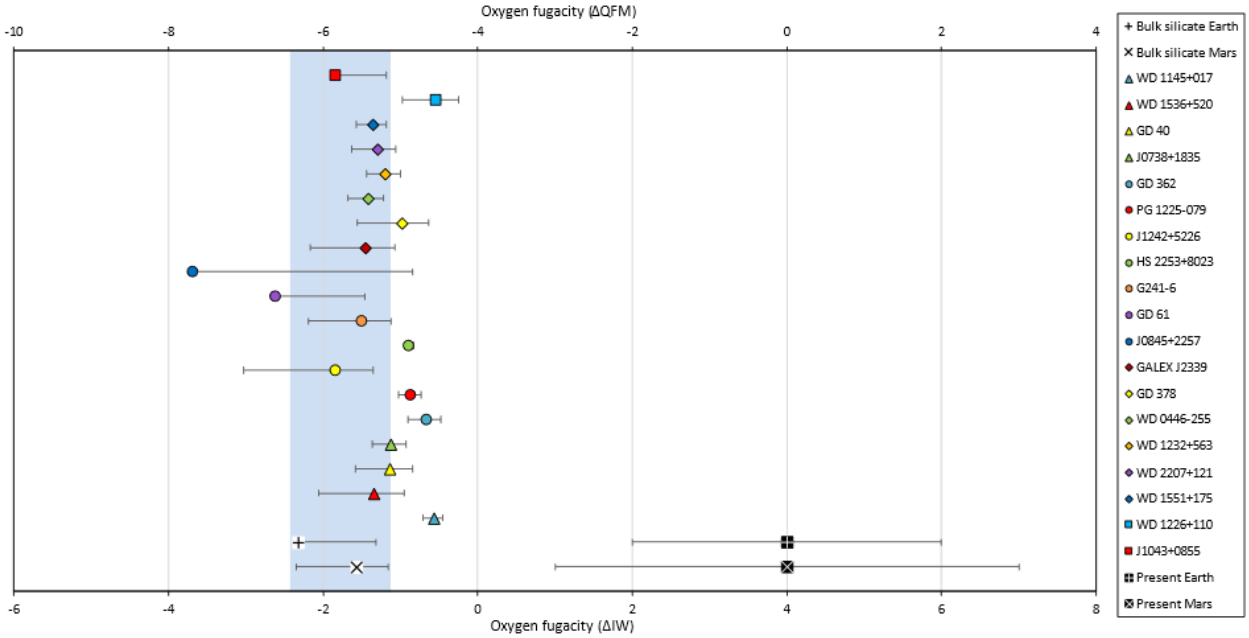

Fig. 5. the oxygen fugacities (fO_2) of polluted white dwarf (WD) stars, bulk silicate Earth (BSE) and bulk silicate Mars (BSM), calculated using the method outlined within this paper. Also included are the average fO_2 values of the present-day upper mantles of Earth (Frost & McCammon 2008) and Mars (Herd et al. 2002). The results are presented in both ΔIW (bottom *x*-axis) and ΔQFM (top *x*-axis).

The triangles represent WDs with helium-dominated atmospheres with data from the Doyle et al. (2019b); the circles represent WDs with helium-dominated atmospheres with data from Harrison et al. (2018); the diamonds represent WDs with helium-dominated atmospheres with data from Doyle (2021); the squares represent WDs with hydrogen-dominated atmospheres with data from Doyle et al. (2019b). The blue column represents the range of fO_2 values estimated for BSE and BSM.

well as the evolution of cyanobacteria in the Proterozoic progressively oxygenated Earth's atmosphere. This theory of early Proterozoic oxidation of the mantle could explain the anoxic, reducing nature of Earth's early atmosphere, as well as the seemingly rapid oxygenation of the atmosphere during the GOE. If this theory is correct, this is also a direct link between the oxidation state (i.e. oxygen fugacity) of a planet's mantle and the atmospheric oxygen concentration of said planet.

Present-day Mars is known to have barely any oxygen within its atmosphere, however the fO_2 values of Earth and Mars' upper mantles are very similar. This may be an indicator that plate tectonics is indeed required for oxidation of the atmosphere: Mars likely exhibited abundant tectonism during its early history, however the more recent climatic history of Mars suggests that this tectonic activity is now significantly reduced (Golombek & Phillips 2010). This may indicate that the volcanism and degassing that possibly allowed for the atmospheric oxygenation of Earth did not occur on Mars, despite the similar upper mantle fO_2 values of these terrestrial planets. In other words, the early tectonism of Mars oxidised the mantle of this planet, however the subsequent decrease in tectonism meant that the atmosphere was not oxygenated.

Many of the WDs within this study have very similar fO_2 values to those of BSE and BSM, implying

Table 2. oxygen fugacities of polluted white dwarf stars calculated within this study.

Object	Temperature (K)	Oxygen fugacity (ΔIW)	Plus error	Minus error
WD 1145+017	16 900	-0.568	0.118	0.136
WD 1536+520	20 800	-1.340	0.387	0.717
GD 40	15 300	-1.140	0.292	0.443
J0738+1835	13 950	-1.120	0.188	0.240
GD 362	10 500	-0.665	0.188	0.241
PG 1225-079	10 800	-0.865	0.132	0.155
J1242+5226	13 000	-1.833	0.485	1.196
HS 2253+8023	14 400	-0.887	0.054	0.057
G241-6	15 300	-1.5	0.378	0.685
GD 61	17 300	-2.62	1.153	--
J0845+2257	19 780	-3.685	2.848	--
GALEX J2339	13 735	-1.454	0.386	0.711
GD 378	15 620	-0.974	0.344	0.579
WD 0446-255	10 120	-1.418	0.203	0.265
WD 1232+563	11 787	-1.189	0.194	0.251
WD 2207+121	14 752	-1.295	0.240	0.333
WD 1551+175	14 756	-1.351	0.174	0.218
WD 1226+110	20 900	-0.536	0.288	0.435
J1043+0855	18 330	-1.840	0.658	--
Bulk silicate Earth	N/A	-2.319	0.818	--
Bulk silicate Mars	N/A	-1.565	0.405	0.783

that the bodies that polluted them shared similar geochemical and geophysical characteristics with the early Earth and Mars. If the parent bodies that polluted these WDs then followed similar evolutionary pathways to that of the Earth (i.e. their mantles became more oxidising and introduced more oxygen into their atmospheres), these parent bodies would have similar atmospheric oxygen conditions to that of Earth at some point

within their history. This could imply that they may have had a similar level of habitability to Earth at some point during their lifetimes, and therefore that it may be beneficial for future stellar observations to search for exoplanets transiting WDs with similar fO_2 values as those in this study.

Following this same line of reasoning, if we were hoping to find exoplanets with lower levels of atmospheric oxygen than the present-day Earth (e.g., those with hypoxic atmospheres, or at least possible hypoxic environments on or below the planet's surface), it may be beneficial to search for WDs with more reducing atmospheres than those of BSE, BSM and the majority of WDs in this study. If a WD has a more reducing initial atmosphere than those of BSE or BSM, and the parent bodies that polluted the star followed a similar evolutionary pathway to Earth, the parent bodies would develop mantles that are more oxidising than their initial states, but less oxidising than the present-day Earth. In other words, their mantles would be oxidising, but less so than that of present Earth's mantle, allowing for the possible development of an hypoxic atmosphere and/or hypoxic environments on the planet.

A possible example of this situation from this study can be seen in fig. 5: J0845+2257 has a more reducing atmosphere than that of BSE, BSM and all other WDs within this study, meaning it is possible that the rocky parent body that polluted this WD may have developed an hypoxic atmosphere during its lifetime. This may therefore have allowed for the development of habitable conditions and possibly complex multicellularity on this body. Of course, the other planetary bodies that polluted the WDs within this study may have developed hypoxic atmospheres during their lifetimes as well, possibly meaning they may have developed multicellular life, however J0845+2257 is the WD within this study that is the likeliest to have had a similar development history to Earth. It should be remembered that the development of an hypoxic atmosphere depends on more than just the initial state of a planet, and factors such as the fluctuating levels of tectonism on the body should also be considered (e.g., see the difference between Earth and Mars). An hypoxic atmosphere may still develop, however, if for example the planet has a less-intense tectonic history than Earth, oxygenating the atmosphere somewhat but to a lesser extent than that of Earth.

This method does of course have limitations. Firstly, it only allows for the calculation of oxygen fugacities of planetary bodies that have already collided with the WDs they previously orbited (i.e. ones that have now been destroyed), thus it is not possible for us to further study these planetary bodies even if they show promising oxygenation levels. However, it is possible that additional planetary bodies continue to orbit the polluted WDs; these bodies may therefore be promising targets for further studies assessing their potential habitability. A second limitation is that fO_2 is not the only factor that determines the atmospheric oxygen content of a planetary body. This is observable by comparing the current oxygen levels of the atmospheres of Earth and Mars: despite having similar upper mantle fO_2 values, Earth and Mars have considerably different atmospheric oxygen levels, 21% for Earth and ~0.174% for Mars (Franz et al. 2017). It can therefore not be immediately assumed that polluted WDs with higher fO_2 values were polluted by exoplanets with high atmospheric O_2; additional factors such as the presence or absence of plate tectonics, or the loss of atmospheric constituents to space, must be considered.

In a similar vein to the point above, whilst this method was successful in identifying that many of the planetary bodies polluting WDs had similar initial geochemical compositions to those of early Earth and Mars, there is no guarantee they would develop in a similar way to Earth or Mars, and therefore there is no guarantee that they ever became habitable. Indeed, even if they developed to become more similar to Mars, this would still mean they would experience extreme environmental conditions, severely reducing their chances of being habitable. Therefore, additional habitability criteria must of course be considered in tandem with oxygen fugacity when studying polluted white dwarfs. Despite these limitations, the identification of the fO_2 values exhibited by these polluted WDs is still an important first step in the search for habitable exoplanets and/or life on worlds beyond our own.

6 Conclusions

Oxygen clearly plays a significant role in the lives of complex multicellular organisms on Earth. It is involved in a large variety of important, energy-producing metabolic processes throughout aerobic respiration, and has long been considered a requirement for the development of life on Earth, as well as on other planets. It is becoming increasingly clear, however, that high levels of oxygen are not necessarily optimal for the development of many forms of complex multicellularity, and in fact cellular hypoxia is required for many key stages in the development process, such as mammalian embryogenesis. The maintenance of cell stemness under hypoxia is an additional important factor in the development cycle of complex multicellular organisms, and as such hypoxia appears to exhibit some level of control over cell and tissue fate, making it an extremely powerful development tool.

Furthermore, hypoxia-inducible transcription factors, which control gene expression under hypoxia, are present within the majority of metazoans, with the

presence of an alternate homologue in vertebrates seemingly representing an increase in the complexity of cellular control during hypoxia. The induction of this HIF homologue seems to produce a state of 'pseudohypoxia' within vertebrates, making organisms 'believe' they are in an hypoxic environment despite this not being true. This allows the organisms to exhibit more complex control of their cellular processes, allowing for increased control of tissue development despite living under the present-day highly oxygenated atmosphere, which generally promotes cellular differentiation, along with the potential production of harmful reactive oxygen species.

The theory of hypoxia being required for life can be expanded to the search for habitable worlds beyond our own. By comparing the oxygen fugacities of polluted white dwarf atmospheres to those of the primitive Earth and Mars, it may be possible to identify the atmospheric oxygen concentration of exoplanets with similar geochemical compositions to our own planet. Furthermore, if we can identify a white dwarf with a more reducing initial composition than that of the primitive Earth, it is possible that the exoplanet polluting this star may have developed an hypoxic atmosphere during its lifetime, and therefore that it was capable of holding life. This is under the assumption that this planet would have a similar lifespan to Earth, and it has an hypoxic atmosphere in the present day, compared to Earth's normoxic one. It is also possible that exoplanets with oxygen fugacities similar to early Earth's could have developed hypoxic atmospheres during their lifetime, even if they do not have one currently. This method has multiple limitations, but it is a possible place to begin the expansion of the search for habitable worlds.

Through experimentation, I found that the expansion of the sedimentary hypoxic niche under an atmosphere of ~10% oxygen was greater within coarser sediment as compared to fine sand, likely due to increased porosity allowing for the more rapid diffusion of oxygen through the sediment. Therefore the development of an hypoxic sedimentary niche is possible even at low levels of atmospheric oxygen, and since hypoxia is required for the emergence and survival of complex life, the search for life elsewhere in the universe should not remain limited to planets with high levels of atmospheric oxygen, but should instead be extended to include those with reduced atmospheric O_2.

To conclude, our understanding of the relationship between oxygen and life is constantly evolving, and it is likely that the current theory of high levels of oxygen being required for the development of complex life is not entirely correct. Instead, further study is required into the relationship between hypoxia and life. This relationship can hopefully be extrapolated to the search for life elsewhere in the universe; however an increased understanding of it would be equally as useful for the study of life here on Earth.

7 Acknowledgements

I would like to thank my supervisors Sylvain Richoz and Emma Hammarlund for their continuous and valuable input regarding this project. I would additionally like to thank Emma in particular for her assistance in the experimental section of this project. Finally, thank you to Per Wahlquist (and Emma Hammarlund once again) for their help with the Swedish version of the abstract for this manuscript.

8 References

Artavanis-Tsakonas, S., Rand, M. D. & Lake, R. J., 1999: Notch signalling: cell fate control and signal integration in development. *Science 284*, 770—776.

Astafieva, M. M., 2019: Archean Fossil Microorganisms. *Paleontological Journal 53*, 228—240.

Bailey-Serres, J. & Voesenek, L. A. C. J., 2008: Flooding stress: acclimations and genetic diversity. *Annual Review of Plant Biology 59*, 313—339.

Bar-On, Y. M., Phillips, R. & Milo, R., 2018: The biomass distribution on Earth. *Proceedings of the National Academy of Sciences of the United States of America 115*, 6506—6511.

Bartlett, R., Elrick, M., Wheeley, J. R., Polyak, V., Desrochers, A. & Asmerom, Y., 2018: Abrupt global-ocean anoxia during the Late Ordovician -early Silurian detected using uranium isotopes of marine carbonates. *Proceedings of the National Academy of Sciences of the United States of America 115,* 5896—5901.

Beckemeyer, R. J. & Hall, J. D., 2007: The entomofauna of the Lower Permian fossil insect beds of Kansas and Oklahoma, USA. *African Invertebrates 48*, 23—39.

Beintema, J. J., Stam, W. T., Hazes, B. & Smidt, M. P., 1994: Evolution of arthropod hemocyanins and insect storage proteins (hexamerins). *Molecular Biology and Evolution 11*, 493—503.

Bekker, A., Holland, H. D., Wang, P.-L., Rumble, D. III, Stein, H. J., Hannah, J. L., Coetzee, L. L. & Beukes, N.J., 2004: Dating the rise of atmospheric oxygen. *Nature 427*, 117—120.

Bell, E. A., Boehnke, P., Harrison, T. M. & Mao, W. L., 2015: Potentially biogenic carbon preserved in a 4.1 billion-year-old zircon. *Proceedings of the National Academy of Sciences of the United States of America 112*, 14518—14521.

Bergman, N. M., Lenton, T. M. & Watson, A. J., 2004: COPSE: A new model of biogeochemical cycling over Phanerozoic time. *American Journal*

of Science 304, 397—437.

Bobrovskiy, I., Hope, J. M., Ivantsov, A., Nettersheim, B. J., Hallmann, C. & Brocks, J. J., 2018: Ancient steroids establish the Ediacaran fossil Dickinsonia as one of the earliest animals. *Science 361*, 1246—1249.

Borgonie, G., Garcia-Moyano, A., Litthauer, D., Bert, W., Bester, A., van Heerden, E., Möller, C., Erasmus, M. & Onstott, T. C., 2011: Nematoda from the terrestrial deep subsurface of South Africa. *Nature 474*, 79—82.

Boutilier, R. G., West, T. G., Pogson, G. H., Mesa, K. A., Wells, J. & Wells, M. J., 1996: Nautilus and the art of metabolic maintenance. *Nature 382*, 534—536.

Brocks, J.J. & Banfield, J., 2009: Unravelling ancient microbial history with community proteogenomics and lipid geochemistry. *Nature Reviews Microbiology 7*, 601—609.

Brouwer, M., Larkin, P., Brown-Peterson, N., King, C., Manning, S. & Denslow, N., 2004: Effects of hypoxia on gene and protein expression in the blue crab, Callinectes sapidus. *Marine Environmental Research 58*, 787—792.

Buick, R., 2008: When did oxygenic photosynthesis evolve?. *Philosophical Transactions: Biological Sciences 363*, 2731—2743.

Buick, R., 2010: Ancient acritarchs. *Nature 463*, 885–886.

Canfield, D. E., 2014: Proterozoic Atmospheric Oxygen. *In* H.D. Holland & K.K. Turekian (eds.): *Treatise on Geochemistry 2nd Edition*, 197—216. Elsevier Science.

Canfield, D. E., 2005: The Early History of Atmospheric Oxygen: Homage to Robert M. Garrels. *Annual Review of Earth and Planetary Sciences 33*, 1—36.

Carpenter, F.M., 1992: Systematic Descriptions of the Superclass Hexapoda, Order Ephemeroptera. *In* R.C. Moore & R.L. Kaesler (eds.): *Treatise on Invertebrate Paleontology. Part R. Arthropoda 4. Hexapoda. Volume 3*, 19—26. The Geological Society of America and The University of Kansas Press, Boulder, Colorado and Lawrence, Kansas.

Carroll, C., Engström, N., Nilsson, P. F., Haxen, E. R., Mohlin, S., Berg, P., Glud, R. N. & Hammarlund, E. U., 2021: Hypoxia generated by avian embryo growth induces the HIF-α response and critical vascularization. *Frontiers in Ecology and Evolution 9*, 1—15.

Case, J. F., 1956: Carbon dioxide and oxygen effects on the spiracles of flies. *Physiological Zoology 29*, 163—171.

Conradi-Larsen, E.-M. & Sømme, L., 1973: Anaerobiosis in the Overwintering Beetle *Pelophila borealis*. *Nature 245*, 388—390.

Crowe, S. A., Døssing, L. N., Beukes, N. J., Bau, M., Kruger, S. J., Frei, R. & Canfield, D. E., 2013: Atmospheric oxygenation three billion years ago. *Nature 501*, 535—539.

Danovaro, R., Dell'Anno, A., Pusceddu, A., Gambi, C., Heiner, I. & Kristensen, R. M., 2010: The first metazoa living in permanently anoxic conditions. *BMC Biology 8*, 30—39.

Dejours, P., 1989: From comparative physiology of respiration to several problems of environmental adaptations and to evolution. *Journal of Physiology 410*, 1—19.

Diaz, R. J. & Rosenberg, R., 2008: Spreading dead zones and consequences for marine ecosystems. *Science 321*, 926—929.

Doyle, A. E., Young, E. D., Klein, B., Zuckerman, B. & Schlichting, H. E., 2019a: Oxygen fugacities of extrasolar rocks: Evidence for an Earth-like geochemistry of exoplanets. *Science 366*, 356—359.

Doyle, A. E., Young, E. D., Klein, B., Zuckerman, B. & Schlichting, H. E., 2019b: Oxygen fugacities of extrasolar rocks: Evidence for an Earth-like geochemistry of exoplanets [supplementary data, Data S1]. *Science 366*.

Doyle, A. E., Young, E. D., Klein, B., Zuckerman, B. & Schlichting, H. E., 2019c: Oxygen fugacities of extrasolar rocks: Evidence for an Earth-like geochemistry of exoplanets [supplementary data, Data S3]. *Science 366*, pp. 24.

Doyle, A. E., 2021: Analyses of polluted white dwarf stars with applications to the geochemistry of rocky exoplanets Ph. D. thesis. University of California, Los Angeles, USA. 223 pp.

Drake, H. & Ivarsson, M., 2018: The role of anaerobic fungi in fundamental biogeochemical cycles in the deep biosphere. *Fungal Biology Reviews 32*, 20—25.

Dufour, P., Kilic, M., Fontaine, G., Bergeron, P., Melis, C. & Bochanski, J., 2012: Detailed compositional analysis of the heavily polluted DBZ white dwarf SDSS J073842.56+183509.06: a window on planet formation?. *The Astrophysical Journal 749*, p. 1—15.

Dupraz, C., Reid, R. P., Braissant, O., Decho, A. W., Norman, R. S. & Visscher, P. T., 2009: Processes of carbonate precipitation in modern microbial mats. *Earth-Science Reviews 96*, 141—162.

El Albani, A., Bengtson, S., Canfield, D. E., Bekker, A., Macchiarelli, R., Mazurier, A., Hammarlund, E. U., Boulvais, P., Dupuy, J.-J., Fontaine, C., Fürsich, F. T., Gauthier-Lafaye, F., Janvier, P., Javaux, E., Ossa, F. O., Pierson-Wickmann, A.-C., Riboulleau, A., Sardini, P., Vachard, D., Whitehouse, M. & Meunier, A., 2010: Large colonial organisms with coordinat-

ed growth in oxygenated environments 2.1 Gyr ago. *Nature 466*, 100—104.

Engel, A. S., 2007: Observations on the biodiversity of sulfidic karst habitats. *Journal of Cave and Karst Studies 69*, 187—206.

Ezashi, T., Das, P. & Roberts, R. M., 2005: Low O2 tensions and the prevention of differentiation of hES cells. *Proceedings of the National Academy of Sciences of the United States of America 102*, 4783—4788.

Farihi, J., Brinkworth, C. S., Gänsicke, B. T., Marsh, T. R., Girven, J., Hoard, D. W., Klein, B. & Koester, D., 2011: Possible signs of water and differentiation in a rocky exoplanetary body. *The Astrophysical Journal Letters 728*, 1—5.

Farihi, J., Koester, D., Zuckerman, B., Vican, L., Gänsicke, B. T., Smith, N., Walth, G. & Breedt, E., 2016: Solar abundances of rock forming elements, extreme oxygen and hydrogen in a young polluted white dwarf. *Monthly Notices of the Royal Astronomical Society 463*, 3186—3192.

Farquhar, J., Zerkle, A. L. & Bekker, A., 2014: Geologic and Geochemical Constraints on Earth's Early Atmosphere *In* H.D. Holland & K.K. Turekian (eds.): *Treatise on Geochemistry, 91—138*. Elsevier.

Forsythe, J. A., Jiang, B.-H., Iyer, N. V., Agani, F., Leung, S. W., Koos, R. D. & Semenza, G. L., 1996: Activation of vascular endothelial growth factor gene transcription by hypoxia-inducible factor 1, *Molecular and Cellular Biology 16*, 4604—4613.

Franz, H. B., Trainer, M. G., Malespin, C. A., Mahaffy, P. R., Atreya, S. K., Becker, R. H., Benna, M., Conrad, P. G., Eigenbrode, J. L., Freissinet, C., Manning, H. L. K., Prats, B. D., Raaen, E. & Wong, M. H., 2017: Initial SAM calibration gas experiments on Mars: Quadrupole mass spectrometer results and implications. *Planetary and Space Science 138*, 44—54.

Frost, D. J. & McCammon, C. A., 2008: The redox state of Earth's mantle. *Annual Review of Earth and Planetary Sciences 36*, 389—420.

Gänsicke, B. T., Koester, D., Farihi, J., Girven, J., Parsons, S. G. & Breedt, E., 2012: The chemical diversity of exo-terrestrial planetary debris around white dwarfs. *Monthly Notices of the Royal Astronomical Society 424*, 333—347.

Geigenberger, P., Fernie, A. R., Gibon, Y., Christ, M. & Stitt, M., 2000: Metabolic activity decreases as an adaptive response to low internal oxygen in growing potato tubers. *Biological Chemistry 381*, 723—740.

Golombek, M. P. & Phillips, R.J., 2010: Mars tectonics. *In* T.R. Watters & R.A. Schultz (eds.): *Planetary Tectonics*, 183—232. Cambridge University Press, New York.

Gooday, A. J., Bernhard, J. M., Levin, L. A. & Suhr, S. B., 2000: Foraminifera in the Arabian Sea oxygen minimum zone and other oxygen-deficient settings: taxonomic composition, diversity, and relation to metazoan faunas. *Deep-Sea Research Part II 47*, 25—54.

Gorr, T. A., Wichmann, D., Hu, J., Hermes-Lima, M., Welker, A. F., Terwilliger, N., Wren, J. F., Viney, M., Morris, S., Nilsson, G. E., Deten, A., Soliz, J. & Gassmann, M., 2010: Hypoxia tolerance in animals: biology and application. *Physiological and Biochemical Zoology 83*, 733—752.

Götz, A., Wani, A. A., Langowski, H.-C., & Wunderlich, J., 2014: Food Storage: Aseptic Packaging. *In* Y. Motarjemi (ed.): *Encyclopedia of Food Safety, Volume 3*, 124—134. Academic Press.

Graham, A. M. & Presnell, J. S., 2017: Hypoxia Inducible Factor (HIF) transcription factor family expansion, diversification, divergence and selection in eukaryotes. *PLOS One 12*, 1—15.

Guintoli, B. & Perata, P., 2014: Transcriptional Regulation Under Low Oxygen Stress in Plants. *In* J.T. van Dongen & F. Licausi (eds.): *Low-Oxygen Stress in Plants, Volume 21, 77—93*. Springer, Vienna.

Guppy, M. & Withers, P., 1999: Metabolic depression in animals: physiological perspectives and biochemical generalizations. *Biological reviews of the Cambridge Philosophical Society 74*, 1—40.

Gustafsson, M. V., Zheng, X., Pereira, T., Gradin, K., Jin, S., Lundkvist, J., Ruas, J. L., Poellinger, L., Lendahl, U. & Bondesson, M., 2005: Hypoxia requires Notch signalling to maintain the undifferentiated cell state. *Developmental Cell 9*, 617—628.

Guzy, R. D. & Schumacker, P. T., 2006: Oxygen sensing by mitochondria at complexIII: the paradox of increased reactive oxygen species during hypoxia. *Experimental Physiology 91*, 807—819.

Halliwell, B. & Gutteridge, J. M. C., 2015: *Free Radicals in Biology and Medicine*. Oxford University Press, New York.

Hallman, C. & Summons, R. E., 2014: Palaeobiological Clues to Early Atmospheric Evolution. *In* H.D. Holland & K.K. Turekian (eds.): *Treatise on Geochemistry*, 139—155. Elsevier.

Hammarlund, E. U., von Stedingk, K. & Påhlman, S., 2018: Refined control of cell stemness allowed animal evolution in the oxic realm. *Nature Ecology & Evolution 2*, 220—228.

Hammarlund, E. U., 2020: Harnessing hypoxia as an evolutionary driver of complex multicellularity.

Interface Focus 10, 1—11.

Harrison, J., Frazier, M. R., Henry, J. R., Kaiser, A., Klok, C. J. & Rascón, B., 2006: Responses of terrestrial insects to hypoxia or hyperoxia. *Respiratory Physiology & Neurobiology 154*, 4—17.

Harrison, J. F., Kaiser, A. & VandenBrooks, J. M., 2010: Atmospheric oxygen level and the evolution of insect body size. *Proceedings: Biological Sciences 277*, 1937—1946.

Harrison, J. H. D., Bonsor, A. & Madhusudhan, N., 2018: Polluted white dwarfs: constraints on the origin and geology of exoplanetary material. *Monthly Notices of the Royal Astronomical Society 000*, 1—34.

Helly, J. J. & Levin, L. A., 2004: Global distribution of naturally occurring marine hypoxia on continental margins. *Deep-Sea Research Part I 51*, 1159—1168.

Herd, C. D. K., Borg, L. E., Jones, J. H. & Papike, J. J., 2002: Oxygen fugacity and geochemical variations in the martian basalts: Implications for martian basalt petrogenesis and the oxidation state of the upper mantle of Mars. *Geochimica et Cosmochimica Acta 66*, 2025—2036.

Hermes-Lima, M. & Zenteno-Savin, T., 2002: Animal response to drastic changes in oxygen availability and physiological oxidative stress. *Comparative Biochemistry and Physiology, Part C 133*, 537—556.

Hetz, S. K. & Bradley, T. J., 2005: Insects breathe discontinuously to avoid oxygen toxicity. *Nature 433*, 516—519.

Hoback, W. W., Podrabsky, J. E., Higley, L. G., Stanley, D. W. & Hand, S. C., 2000: Anoxia tolerance of con-familial tiger beetle larve is associated with differences in energy from and anaerobiosis. *Journal of Comparative Physiology B 170*, 307—314.

Hoback, W. W. & Stanley, D. W., 2001: Insects in hypoxia. *Journal of Insect Physiology 47*, 533—542.

Hochachka, P. W., Nener, J. C., Hoar, J. & Saurez, R. K., 1993: Disconnecting metabolism from adenylate control during extreme oxygen limitation. *Canadian Journal of Zoology 71*, 1267—1270.

Holland, H. D., 1984: *The Chemical Evolution of the Atmosphere and Oceans*. Princeton University Press, New Jersey.

Holland, H. D., 2006: The oxygenation of the atmosphere and oceans. *Philosophical Transactions: Biological Sciences 361*, 903—915.

Hourdez, S., 2012: Hypoxic Environments. *In* E.M. Bell (ed.): *Life at Extremes: Environments, Organisms and Strategies for Survival*. CAB International, Wallingford.

Iyer, N. V., Kotch, L. E., Agani, F., Leung, S. W., Laughner, E., Wenger, R. H., Gassmann, M., Gearhart, J. D., Lawler, A. M., Yu, A. Y. & Semenza, G. L. , 1998: Cellular and developmental control of O2 homeostasis by hypoxia-inducible factor 1α. *Genes & Development 12*, 149—162.

Jebaraj, C. S., Raghukumar, C., Behnke, A. & Stoeck, T., 2010: Fungal diversity in oxygen-depleted regions of the Arabian Sea revealed by targeted environmental sequencing combined with cultivation. *FEMS Microbiology Ecology 71*, 399—412.

Joanisse, D. R. & Storey, K. B., 1998: Oxidative stress and antioxidants in stress and recovery of cold-hardy insects. *Insect Biochemistry and Molecular Biology 28*, 23—30.

Jura, M., Xu, S., Klein, B., Koester, D. & Zuckerman, B., 2012: Two extrasolar asteroids with low volatile-element mass fractions. *The Astrophysical Journal 750*, 1—12.

Kallmeyer, J., Pockalny, R., Adhikari, R. R., Smith, D. C. & D'Hondt, S., 2012: Global distribution of microbial abundance and biomass in subseafloor sediment. *Proceedings of the National Academy of Sciences of the United States of America 109*, 16213—16216.

Kamykowski, D. & Zentara, S.-J., 1990: Hypoxia in the world ocean as recorded in the historical data set. *Deep-Sea Research 37*, 1861—1874.

Kasting, J. F., Eggler, D. H. & Raeburn, S. P., 1993: Mantle redox evolution and the oxidation state of the Archaean atmosphere. *The Journal of Geology 101*, 245—257.

Kieft, T. L., 2016: Microbiology of the Deep Continental Biosphere *In* C.J. Hurst (ed.): *Their World: A Diversity of Microbial Environments*, 225—250. Springer, Switzerland.

King, T. C., 2007: Cell Injury, Cellular Responses to Injury, and Cell Death. *In* A. Stibbe & A. Hall (eds.): *Elsevier's Integrated Pathology*, 1—20. Mosby, Inc., Philadelphia, Pennsylvania.

Klein, B., Jura, M., Koester, D. & Zuckerman, B., 2011: Rocky extrasolar planetary compositions derived from externally polluted white dwarfs. *The Astrophysical Journal 741*, 1—18.

Klein, B., Doyle, A. E., Zuckerman, B., Dufour, P., Blouin, S., Melis, C., Weinberger, A. J. & Young, E. D., 2021: Discovery of beryllium in white dwarfs polluted by planetesimal accretion. *arXiv: 2102.01834*, 23 pp.

Knoll, A. H., 2011: The multiple origins of complex multicellularity. *The Annual Review of Earth and Planetary Sciences 39*, 217—239.

Knoll, A. H. & Carroll, S. B., 1999: Early animal evolution: emerging views from comparative biolo-

gy and geology. *Science 284*, 2129—2137.
Lee, P., Chandel, N. S. & Simon, M. C., 2020: Cellular adaptation to hypoxia through hypoxia inducible factors and beyond. *Nature Reviews. Molecular Cell Biology 21*, 268—283.
Levin, L. A., 2003: Oxygen Minimum Zone benthos: adaptation and community response to hypoxia. *Oceanography and Marine Biology 41*, 1—45.
Licausi, F., Kosmacz, M., Weits, D. A., Giuntoli, B., Giorgi, F. M., Voesenek, L. A. C. J., Perata, P. & van Dongen, J. T., 2011: Oxygen sensing in plants is mediated by an N-end rule pathway for protein destabilization. *Nature 479*, 419—423.
Lighton, J. R. B., 1996: Discontinuous gas exchange in insects. *Annual Review of Entomology 41*, 309—324.
Lighton, J. R. B., 1998: Notes from underground: towards ultimate hypotheses of cyclic, discontinuous gas-exchange in tracheate arthropods. *American Zoologist 38*, 483—491.
Lindmark, D. G. & Müller, M., 1973: Hydrogenosome, a cytoplasmic organelle of the anaerobic flagellate Trichomonas foetus, and its role in pyruvate metabolism. *The Journal of Biological Chemistry 248*, 7724—7728.
Liu, Y., Cox, S. R., Morita, T. & Kourembanas, S., 1995: Hypoxia regulates vascular endothelial growth factor gene expression in endothelial cells. Identification of a 5' Enhancer. *Circulation Research 77*, 638—643.
Loudon, C., 1989: Tracheal hypertrophy in mealworms: design and plasticity in oxygen supply systems. *Journal of Experimental Biology 147*, 217—235.
Lyons, T. W., Reinhard, C. T. & Planavsky, N. J., 2014: The rise of oxygen in Earth's early ocean and atmosphere. *Nature 506*, 307—315.
Maltepe, E., Schmidt, J. V., Baunoch, D., Bradfield, C. A. & Simon, M. C., 1997: Abnormal angiogenesis and responses to glucose and oxygen deprivation in mice lacking the protein ARNT. *Nature 386*, 403-407.
McCord, J. M., Keele, B. B. Jr. & Fridovich, I., 1971: An enzyme-based theory of obligate anaerobiosis: the physiological function of superoxide dismutase. *Proceedings of the National Academy of Sciences of the United States of America 68*, 1024—1027.
McDonough, W. F., 2003: Compositional Model for the Earth's Core. *In* H.D. Holland & K.K. Turekian (eds.): *Treatise on Geochemistry*, 547—568. Elsevier.
McMahon, S. & Parnell, J., 2014: Weighing the deep continental biosphere. *FEMS Microbiology Ecology 87*, 113—120.
McMahon, S. & Parnell, J., 2018: The deep history of Earth's biomass. *Journal of the Geological Society 175*, 716—720.
Meadows, V. S., Reinhard, C. T., Arney, G. N., Parenteau, M. N., Schwieterman, E. W., Domagal-Goldman, S. D., Lincowski, A. P., Stapelfeldt, K. R., Rauer, H., DasSarma, S., Hegde, S., Narita, N., Deitrick, R., Lustig-Yaeger, J., Lyons, T. W., Siegler, N. & Grenfell, J. L., 2018: Exoplanet biosignatures: Understanding oxygen as a biosignature in the context of its environment. *Astrobiology 18*, 630—662.
Melis, C. & Dufour, P., 2017: Does a differentiated, carbonate-rich, rocky object pollute the white dwarf SDSS J104341.53+085558.2?. *The Astrophysical Journal 834*, 1—9.
Melton, D., 2013: "Stemness": Definitions, Criteria, and Standards. *In* R. Lanza & A. Atala (eds.): *Handbook of Stem Cells, Volume 1: Pluripotent Stem Cells*. Elsevier Inc. 1040 pp.
Mills, D. B., Ward, L. M., Jones, C., Sweeten, B., Forth, M., Treusch, A. H., & Canfield, D. E., 2014: Oxygen requirements of the earliest animals. *Proceedings of the National Academy of Sciences of the United States of America 111*, 4168—4172.
Montgomery, M. H., Thompson, S. E. & von Hippel, T., 2008: Constraining the surface inhomogeneity and settling times of metals on accreting white dwarfs. *The Astrophysical Journal 685*, 1—4.
Morriss, G. M. & New, D. A. T., 1979: Effect of oxygen concentration on morphogenesis of cranial neural folds and neural crest in cultured rat embryos. *Journal of Embryology and Experimental Morphology 54*, 17—35.
Mukhopadhyay, C. K., Mazumder, B. & Fox, P. L., 2000: Role of hypoxia-inducible factor-1 in transcriptional activity of ceruloplasmin by iron deficiency. *The Journal of Biological Chemistry 275*, 21048—21054.
Mukhopadhyay, J., Crowley, Q. G., Ghosh, S., Ghosh, G., Chakrabarti, K., Misra, B., Heron, K. & Bose, S., 2016: Oxygenation of the Archaean atmosphere: New paleosol constraints from eastern India. *Geology 42*, 923—926.
Mustroph, A., Hess, N. & Sasidharan, R., 2014: Hypoxic Energy Metabolism and PPi as an Alternative Energy Currency. *In* J.T. van Dongen & F. Licausi (eds.): *Low-Oxygen Stress in Plants, Volume 21*, 165—184. Springer, Vienna.
Nursall, J. R., 1959: Oxygen as a prerequisite to the origin of the metazoa. *Nature 183*, 1170—1172.
Nutman, A. P., Bennett, V. C., Friend, C. R. L., Van Kranendonk, M. J., & Chivas, A. R., 2016: Rapid emergence of life shown by discovery of 3,700-million-year-old microbial structures.

Nature 537, 535—538.
Ohmoto, Y., Kakegawa, T., Ishida, A., Nagase, T. & Rosing, M. T., 2014: Evidence for biogenic graphite in early Archaean Isua metasedimentary rocks. *Nature Geoscience 7*, 25—28.
Pinti, D. L., 2014: Bulk Silicate Earth. *In* M. Gargaud, W. M. I., R. Amils, H.J. Cleaves, P. Daniele, J.C. Quintanilla & M. Viso (eds.): *Encyclopedia of Astrobiology*. Springer, Berlin.
Raddi, R., Gänsicke, B. T., Koester, D., Farihi, J., Hermes, J. J., Scaringi, S., Breedt, E. & Girven, J., 2015: Likely detection of water-rich asteroid debris in a metal-polluted white dwarf. *Monthly Notices of the Royal Astronomical Society 450*, 2083—2093.
Reiling, J.H. & Hafen, E., 2004: The hypoxia-induced paralogs Schylla and Charybdis inhibit growth by down-regulating S6K activity upstream of TSC in Drosophila. *Genes & Development 18*, 2879—2892.
Reipschläger, A. & Portner, H. O., 1996: Metabolic depression during environmental stress: the role of extracellular versus intracellular pH in Sipunculus nudus. *The Journal of Experimental Biology 199*, 1801—1807.
Richter, D. J., Fozouni, P., Eisen, M. B. & King, N., 2018: Gene family innovation, conservation and loss on the animal stem lineage. *eLife 7*, 1—43.
Robbins, E. I., Porter, K. G. & Haberyan, K. A., 1985: Pellet microfossils: Possible evidence for metazoan life in Early Proterozoic time. *Proceedings of the National Academy of Sciences of the United States of America 82*, 5809—5813.
Rodesch, F., Simon, P., Donner, C. & Jauniaux, E., 1992: Oxygen measurements in endometrial and trophoblastic tissues during early pregnancy. *Obstetrics and Gynecology 80*, 283—285.
Rolfs, A., Kvietikova, I., Gassmann, M. & Wenger, R. H., 1997: Oxygen-regulated transferrin expression is mediated by hypoxia-inducible factor-1. *The Journal of Biological Chemistry 272*, 20055—20062.
Rosing, M. T. & Frei, R., 2004: U-rich Archaean sea-floor sediments from Greenland – indications of >3700 Ma oxygenic photosynthesis. *Earth and Planetary Science Letters 217*, 237—244.
Schaefer, L. & Fegley, B. Jr., 2017: Redox states of initial atmospheres outgassed on rocky planets and planetesimals. *The Astrophysical Journal 843*, 1—18.
Schmidt-Rohr, K., 2020: Oxygen is the high-energy molecule powering complex multicellular life: Fundamental corrections to traditional bioenergetics. *ASC Omega 5*, 2221—2233.
Semenza, G. L., 2007: Life with Oxygen. *Science 318*, 62—64.
Semenza, G. L. & Wang, G. L., 1992: A nuclear factor induced by hypoxia via de novo protein synthesis binds to the human erythropoietin gene enhancer at a site required for transcriptional activation. *Molecular and Cellular Biology 12*, 5447—5454.
Shoshani, T., Faerman, A., Mett, I., Zelin, E., Tenne, T., Gorodin, S., Moshel, Y., Elbaz, S., Budanov, A., Chajut, A., Kalinski, H., Kamer, I., Skaliter, R. & Feinstein, E., 2002: Identification of a novel hypoxia-inducible factor 1-responsive gene, RTP801, involved in apoptosis. *Molecular and Cellular Biology 22*, 2283—2293.
Shweiki, D., Itin, A., Soffer, D. & Keshet, E., 1992: Vascular endothelial growth factor induced by hypoxia may mediate hypoxia-induced angiogenesis. *Nature 359*, 843—845.
Simon, M. C. & Keith, B., 2008: The role of oxygen availability in embryonic development and stem cell function. *Nature Reviews Molecular Cell Biology 9*, 285—296.
Sperling, E. A., Halverson, G. P., Knoll, A. H., Macdonald, F. A., & Johnston, D. T., 2013: A basin redox transect at the dawn of animal life. *Earth and Planetary Science Letters 371—372*, 143—155.
Stevens, T., 1997: Lithoautotrophy in the subsurface. *FEMS Microbiology Reviews 20*, 327—337.
Swan, A., Farihi, J., Koester, D., Hollands, M., Parsons, S., Cauley, P. W., Redfield, S. & Gänsicke, B. T., 2019: Interpretation and diversity of exoplanetary material orbiting white dwarfs. *Monthly Notices of the Royal Astronomical Society 490*, 202—218.
Takai, K., Nakamura, K., Toki, T., Tsunogai, U., Miyazaki, M., Miyazaki, J., Hirayama, H., Nakagawa, S., Nunoura, T. & Horikoshi, K., 2008: Cell proliferation at 122°C and isotopically heavy CH4 production by a hyperthermophilic methanogen under high-pressure cultivation. *Proceedings of the National Academy of Sciences of the United States of America 105*, 10949—10954.
Taylor, G. J., 2013: The bulk composition of Mars. *Chemie der Erde 73*, 401—420.
Thompson, J. B., Mullins, H. T., Newton, C. R. & Vercoutere, T. L., 1985: Alternative biofacies model for dysaerobic communities. *Lethaia 18*, 167—179.
Turner, S., Huang, T.-C., & Chaw, S.-M., 2001: Molecular phylogeny of nitrogen-fixing unicellular cyanobacteria. *Botanical Bulletin of Academia Sinica 42*, 181—186.
Turner, E. C., 2021: Possible poriferan body fossils in early Neoproterozoic microbial reefs. *Nature 596*, 87—91.

Van Nerum, K. & Buelens, H., 1997: Hypoxia-controlled winter metabolism in honeybees (Apis mellifera). *Comparative Biochemistry and Physiology 117A*, 445—455.

Voesenek, L. A. C. J., Banga, M., Thier, R. H., Mudde, C. M., Harren, F. J. M., Barendse, G. W. M. & Blom, C. W. P. M., 1993: Submergence-induced ethylene synthesis, entrapment, and growth in two place species with contrasting flooding resistances. *Plant Physiology 103*, 783—791.

Wang, Z., Liu, Y., Zong, K., Lin, J. & Kusky, T. M., 2020: Mantle degassing related to changing redox and thermal conditions during the Precambrian supercontinent cycle. *Precambrian Research 350*, 1—11.

Weinert, D. J., 2009: Nutrition and muscle protein synthesis: a descriptive review. *The Journal of the Canadian Chiropractic Association 53*, 186—193.

Wenger, R. H., 2002: Cellular adaptation to hypoxia: O2-sensing protein hydroxylases, hypoxia-inducible transcription factors, and O2-regulated gene expression. *The FASEB Journal 16*, 1151—1162.

Wetzel, D. T., Rutherford, M. J., Jacobsen, S. D., Hauri, E. H. & Saal, A. E., 2013: Degassing of reduced carbon from planetary basalts. *Proceedings of the National Academy of Sciences of the United States of America 110*, 8010—8013.

Whitman, W. B., Coleman, D. C. & Wiebe, W. J., 1998, Prokaryotes: The unseen majority. *Proceedings of the National Academy of Sciences of the United States of America 95*, 6578—6583.

Wigglesworth, V. B., 1935: The regulation of respiration in the flea, Xenopsylla cheopis, Roths. (Pulicidae). *Proceedings of the Royal Society of London. Series B, Biological Sciences 118*, 397—419.

Wilson, D. J., Gänsicke, B. T., Koester, D., Toloza, O., Pala, A. E., Breedt, E. & Parsons, S. G., 2015: The composition of a disrupted extrasolar planetesimal at SDSS J0845+2257 (Ton 345). *Monthly Notices of the Royal Astronomical Society 451*, 3237—3248.

Wykoff, C. C., Beasley, N. J. P., Watson, P. H., Turner, K. J., Pastorek, J., Sibtain, A., Wilson, G. D., Turley, H., Talks, K. L., Maxwell, P. H., Pugh, C. W., Ratcliffe, P. J. & Harris, A. L., 2000: Hypoxia-inducible expression of tumor-associated carbonic anhydrases. *Cancer Research 60*, 7075—7083.

Xu, S., Jura, M., Klein, B., Koester, D. & Zuckerman, B., 2013: Two beyond-primitive extrasolar planetesimals. *The Astrophysical Journal 766*, 1—14.

Xu, S., Jura, M., Dufour, P. & Zuckerman, B., 2016: Evidence for gas from a disintegrating extrasolar asteroid. *The Astrophysical Journal Letters 816*, 1—6.

Xu, S., Dufour, P., Klein, B., Melis, C., Monson, N. N., Zuckerman, B., Young, E. D. & Jura, M. A., 2019: Compositions of planetary debris around dusty white dwarfs. *The Astronomical Journal 158*, 1—17.

Yamaguchi, Y. & Miura, M., 2013: How to form and close the brain: insight into the mechanism of cranial neural tube closure in mammals. *Cellular and Molecular Life Sciences 70*, 3171—3186.

Yin, L., Meng, F., Kong, F. & Niu, C., 2020: Microfossils from the Paleoproterozoic Hutuo Group, Shanxi, North China: Early evidence for eukaryotic metabolism. *Precambrian Research 342*, 1—10.

Zebe, B., 1991: Arthropods. *In* C. Bryant (ed.): *Metazoan Life without Oxygen*, 218—237. St. Edmundsbury Press, Bury St Edmunds

Zhang, S., Wang, X., Wang, H., Bjerrum, C. J., Hammarlund, E. U., Mafalda Costa, M., Connelly, J. N., Zhang, B., Su, J. & Canfield, D. E., 2016: Sufficient oxygen for animal respiration 1,400 million years ago. *Proceedings of the National Academy of Sciences of the United States of America 113*, 1731—1736.

Appendix A – Additional background information

A.1 — Arguments against the link between insect gigantism and hyperoxia

The evidence for insect gigantism during the Carboniferous Period is based on just a few documented fossils, hence the concept of gigantic insects during periods of hyperoxia may just be a sampling artefact. Similarly, extant insect species represent just a small fraction of all species that have ever lived, so it is not necessarily unusual that larger species existed in the past. There is also the possibility that these giant insects were outliers to the general pattern of insect body sizes, and not the norm; in fact plots of insect size distribution during the Permo-Carboniferous indicate that the majority of insects around this time were not giant. For example, Beckemeyer & Hall (2007) found that most insects of the Wellington Formation of Lower Permian age had forewings <25 mm in length (see fig. 9 of Beckemeyer & Hall 2007). Harrison et al. (2010) acknowledge that the largest insects of the Permo-Carboniferous were certainly larger than during any other time period, however it is unknown whether average insect size was increased during this period (corroborating the theory that this insect gigantism may be a taphonomic artefact, preserving only the largest of a generally small group). Linking this possible gigantism back to hyperoxia, there is possible evidence for insect gigantism also during the Cretaceous Period, for example among certain families of mayfly (Carpenter 1992). However, it is still debated whether the atmosphere was hypoxic or hyperoxic during this period (Harrison et al. 2010), and thus it is unclear whether the presence of these giant insects supports or disproves the theory of hyperoxia causing insect gigantism.

A.2 — HIF homologues in plants

Groups other than animals are not currently known to have evolved HIF homologues. However, other hypoxia-response mechanisms are known to exist within plant species. Many plants are known to experience periods of submergence due to flooding; this submergence is often accompanied by reduced oxygen levels, which has been shown to lead to the build-up of the hormone molecule ethylene within plant tissues (e.g., Voesenek et al. 1993). Subsequently, adaptations to these submergence conditions are known to take place within various species, and are also known to be driven by ethylene-response factors (ERFs, e.g., Bailey-Serres & Voesenek 2008). These ERFs are transcription factors which alter their rate of protein transcription in relation to the concentration of ethylene within plant tissues, and many of them have been investigated regarding their role in the hypoxic response of plants. It was subsequently found that a specific group of ERFs can be regulated post-translationally by oxygen (Guintoli & Perata 2014). This means that, under normoxia, this group of ERFs can be prevented from accumulating in the nucleus (Licausi et al. 2011), and therefore prevented from control of gene expression. When hypoxic conditions are encountered, these ERFs are relocated to the nucleus of plant cells, where they begin the transcription of proteins to be utilised in the hypoxic response. A specific example of an ERF within this group is RAP2.12, a transcription factor that is constitutively expressed within cells of *Arabidopsis thaliana* (Licausi et al. 2011). Under normoxic conditions, RAP2.12 is stored in the plasma membrane of cells. When the plant is subjected to hypoxia, this ERF is rapidly transported to the nucleus of the cell, to promote the transcription of proteins involved in the hypoxic response (Licausi et al. 2011).

A.3 — HIF target genes in animals

Perhaps the most prominent example of a target gene for HIF-1 is VEGF (vascular endothelial growth factor), a gene involved in the formation of blood vessels. It was first discovered in the 1990s that VEGF expression was up-regulated during hypoxia (Shweiki et al. 1992). The result of this up-regulation was the production of 'collateral' blood vessels adjacent to hypoxic tissues (Shweiki et al. 1992), allowing for the increased supply of oxygenated blood to the areas affected by hypoxia. Whilst there was no mention of HIF within this paper, in the years following this initial discovery multiple authors identified the involvement of HIF-1 in the up-regulation of VEGF during hypoxia (Liu et al. 1995; Forsythe et al. 1996). Multiple additional examples of HIF-1 target genes that are up-regulated during hypoxia exist. Ceruloplasmin increases the oxidation of iron from ferrous to ferric molecular species, and is up-regulated 5–10-fold during hypoxia (Mukhopadhyay et al. 2000). These ferric species can then be bound by transferrin (Wenger 2002), the increased production of which enhances the transport of iron to blood cells (Rolfs et al. 1997). Furthermore, transmembrane carbonic anhydrases convert protons and bicarbonate to carbon dioxide to regulate pH (Wenger 2002). This final example is especially important as the switch to anaerobic respiration is common during hypoxia, and this can lead to the increased production of lactate, which in turn can cause a decrease in extracellular pH (Wykoff et al. 2000). This may result in adverse effects for the organism in question, and therefore the upregulation of carbonic anhydrases is essential for the maintenance of an appropriate pH level under hypoxia. These examples all therefore outline the importance of HIF as a mediator of gene regulation in the

hypoxic response.

Another example of a HIF target within animals is the Notch signalling pathway. Notch is a signalling cascade which controls cell fate (e.g., differentiation, proliferation, apoptosis) within multicellular organisms (Artavanis-Tsakonas et al. 1999; Simon & Keith 2008). Gustafsson et al. (2005) proved that Notch signalling is required for the maintenance of the undifferentiated cell state under hypoxia. Furthermore, HIF-1α work in tandem with the Notch pathway to promote the undifferentiated cell state in multicellular organisms: HIF-1α binds to a hypoxia response element of a gene within the Notch signalling pathway, which promotes the expression of genes downstream within the pathway. This already shows how important Notch signalling is for the development of multicellular organisms, maintaining the stem cell population that is required for the generation and renewal of complex tissues (Hammarlund et al. 2018). However, what is even more interesting about Notch signalling is that it appears to be evolutionarily preserved. It was originally thought that the Notch gene family was unique to animals, however genes within the Notch pathway have since been identified in choanoflagellate (protist) genomes (Richter et al. 2018), implying that this pathway has existed since before the divergence of choanoflagellates and metazoans. HIFs are also thought to be restricted to metazoans (Graham & Presnell 2017); however, the presence of Notch signalling in choanoflagellates (the closest known evolutionary relatives of metazoans) could suggest the presence of HIFs within this group also. This could further imply that hypoxic control of cell fate was also present within this group, making it a more ancient evolutionary trait than previously realised.

As a specific example of hypoxic control of gene expression, we will look at the expression of two genes of the fruit fly *Drosophila*. All information for this paragraph is from Reiling & Hafen (2004), unless otherwise stated. The genes *scylla* and *charybdis* are largely dispensable for *Drosophila* under normoxia, however they appear to have a critical role in the endurance of prolonged hypoxia. Both of these genes have been shown to be up-regulated during hypoxia, and the removal of both genes from *Drosophila* makes individuals more susceptible to negative effects of reduced oxygen conditions. In addition to this, individuals lacking both genes showed increased physical growth, and those with both genes exhibited reduced growth. These genes reduce cell growth by reducing phosphorylation of the ribosomal protein S6, which reduces cell size, but not number. The *scylla* gene also has a mammalian counterpart, *RTP801*, the up-regulation of which was discovered to have differing effects depending on the cellular context. When up-regulated by hypoxia, it appeared to reduce the production of reactive oxygen species, therefore protecting certain cells from apoptosis, specifically MCF7 (human breast carcinoma) and PC12 (rat adrenal tumour) cells (Shoshani et al. 2002). However, the up-regulation of this gene induced toxic effects in differentiated, neuron-like PC12 cells (also sourced from rat adrenal tumours), along with increasing the sensitivity of these cells to oxidative or ischemic damage (Shoshani et al. 2002), the latter of which is due to reduced blood flow and can cause cellular injuries such as rapid acidosis or cellular dysfunction (King 2007). The up-regulation of this gene appears to only be toxic to non-dividing types of PC12 cells (Shoshani et al. 2002), perhaps suggesting a role for hypoxia in the maintenance of populations of dividing cells. This further indicates the importance of hypoxia within the development of multicellular life.

Hypoxia does not just trigger the up-regulation of certain genes; down-regulation is also a common feature of the hypoxic response. For example, it was found that the blue crab *Callinectes sapidus*, when exposed to five days of hypoxia (2–3 ppm dissolved oxygen), down-regulates the expression of several genes that code for proteins including manganese-dependent superoxide dismutase (MnSOD), hemocyanin, and the ribosomal genes S15 and L23 (Brouwer et al. 2004). The latter two of these proteins are ribosomes, helping to produce more proteins (Brouwer et al. 2004), but the former two proteins are involved in the fate of oxygen within the body: hemocyanin transports oxygen through the body of many invertebrates (Beintema et al. 1994), whilst MnSOD catalyses the partitioning of superoxide radicals into molecular oxygen and hydrogen peroxide (McCord et al. 1971). Superoxide radicals are a type of reactive oxygen species (ROS), which have the capacity to cause many pathological conditions within organisms (e.g., Hermes-Lima & Zenteno-Savin 2002; Halliwell & Gutteridge 2015). Therefore, the reduced expression of these proteins would result in decreased synthesis of additional proteins, decreased oxygen transport within the organism, and decreased breakdown of superoxide radicals respectively. Whilst on the surface the down-regulation of all of these genes seems to be a response by the organism to hypoxic stress (Brouwer et al. 2004), another possibility is that it suggests a reduction in metabolic activity in response to hypoxia. With decreased ambient O_2, there is less oxygen to be transported throughout the body, hence the down-regulation of hemocyanin. Additionally, fewer superoxide radicals would be produced, so there would be less use for MnSOD. Finally, protein synthesis is an energy-intensive process (e.g. Weinert 2009), and thus reducing protein synthesis would conserve energy under lower oxygen conditions. Brouwer et al. (2004) also concluded that the down-regulation of hemocyanin is an indicator that *C. sapidus* shuts down its aerobic metabolism after five days of exposure to hypoxia. This may provide evidence that the down-regulation of certain proteins during hypoxia is a viable technique for the conservation of energy and the reduction of metabolic rate.

A.4 — Metabolic rate reduction in plants and animals

It was found that hypoxia is an active factor used to control MR in hibernating honeybee clusters (Van Nerum & Buelens 1997). The studied bees within a hibernating cluster were able to control their metabolic rate through control of the oxygen level within the cluster – a permanent O_2 level of ~15% was observed within the cluster during multiple winter periods, with the bees exhibiting a reduced MR as a technique for the conservation of energy (Van Nerum & Buelens 1997). A further reduction to a state of ultra-low MR was also present within the cluster. This ultra-low MR state involved absolute immobility and a lack of temperature control, and was observed to be optional at 15% O_2, before becoming compulsory at ~7.5% O_2 (Van Nerum & Buelens 1997). This hypoxia control and subsequent reduction of MR serves to significantly reduce the energy requirements of the honeybees during hibernation, presumably allowing them to conserve energy use after the hibernation period.

Suppression of MR in response to reduced O_2 has also been observed in other groups of insects. It was found that the larvae of the tiger beetle *Cicindela togata* can survive up to 5 days of anoxia through suppressing their MR by 97% of normoxic levels (i.e. the larvae operate at 3% of normoxic levels; Hoback et al. (2000)). This, combined with the simultaneous downregulation of heat dissipation to 3.4%, allows for the maintenance of normoxic levels of ATP (adenosine triphosphate, the breakdown of which provides energy for most metabolic processes) for up to 24 hours (Hoback et al. 2000). This response appears to have developed as a result of the flooding risk of the environments in which *C. togata* commonly lives. In a similar situation, the desert locust *Schistocerca gregaria* can survive for up to 8 hours under anoxia by entering a state of dormancy, and reducing MR to 6–7% of normoxic levels (Hochachka et al. 1993). The locusts are also then able to recover from this dormant state when the environment is reoxygenated by increasing their MR to above the rates initially observed at normoxia, until the 'oxygen debt' brought on by the anoxia is cleared (Hoback & Stanley 2001).

The reduction of MR under reduced oxygen conditions is not exclusive to terrestrial animals; this trait is commonly observed in marine organisms as well. For example, the cephalopod *Nautilus pompilius* depresses its aerobic metabolic rate to 4–8% of normoxic levels when travelling through severely hypoxic waters (Boutilier et al. 1996). Furthermore, the marine worm *Sipunculus nudus* has been shown to exhibit metabolic depression in response to the reduction of extracellular pH, which itself was a result of hypoxia (Reipschläger & Pörtner 1996). The suppression of MR is also not exclusive to the animal kingdom itself; plants have been shown to utilise similar methods when exposed to hypoxic conditions. Geigenberger et al. (2000) observed the extensive inhibition of several metabolic processes (including glycolysis, respiration and the breakdown of sucrose) within potato tuber discs exposed to 4% O_2. In contrast, an opposite pattern occurred under anoxia, with the doubling of glycolysis, along with the increased production of starch and lactate. It was therefore concluded that decreased (but not completely depleted) internal oxygen conditions within potato tubers resulted in the decreased consumption of ATP, through the reduction of metabolic activity and a switch to less ATP-intensive pathways (Geigenberger et al. 2000). The same authors measured hypoxia (<5% O_2) at the centre of potato tubers that were growing in 18% ambient O_2 at 20°C. This introduces the possibility that hypoxia is common within the growing stages of potato tubers (and possibly other clades), and therefore that the reduction of MR is a common response to hypoxia within many types of organisms, and is not exclusive to animals.

A.5 — Utilisation of anaerobic metabolic pathways

One substrate possibly utilised during anaerobic respiration is trehalose, a carbohydrate composed of two glucose molecules (Zebe 1991). It is likely that trehalose is utilised by the larvae of many aquatic insects under hypoxic/anoxic conditions (Zebe 1991), and thus Hoback et al. (2000) concluded this molecule to be a likely substrate for the larvae of both *C. togata* and another species of tiger beetle (*Amblycheila cylindriformis*) during anoxia. This would initially suggest that both species would be able to perform similarly well during reduced oxygen conditions, however it was found that *C. togata* was able to maintain ATP levels equal to those seen under normoxia for up to 72 hours of anoxia exposure, and *A. cylindriformis* was not (Hoback et al. 2000). The authors found these performance differences to correlate with the flooding risk of the environments in which the species lived, as well as the distribution of these species (Hoback et al. 2000): the habitats of *C. togata* experience seasonal flooding (and therefore anoxia), whereas those of *A. cylindriformis* do not. A similar example comes in the form of the adult ground beetle *Pelophila borealis*. These organisms are frequently exposed to anoxic conditions during the winter, when they are buried under sediment which is then subsequently flooded and covered by a layer of ice (Conradi-Larsen & Sømme 1973). Experimental data revealed that these beetles exhibited close to 100% survival for up to 127 days in anoxia (Conradi-Larsen & Sømme 1973). It was also found that common products of anaerobic respiration, such as lactate and alanine, increased in abundance with increased storage time in anoxia. Additionally, individuals that

were returned from anoxia to normoxia after 49 days exhibited an increased level of oxygen consumption compared to those that were not kept in anoxia at all. This 'oxygen debt' is thought to be caused by the oxidation of metabolites during anaerobiosis (Conradi-Larsen & Sømme 1973), which when combined with the other evidence presented above is proof that anaerobic respiration has taken place. These examples outline both the importance of utilising alternative metabolic pathways during reduced oxygen conditions, as well as the power of evolution and adaptation in the response to fluctuating oxygen levels.

The utilisation of anaerobic metabolic pathways and alternative energy-providing substrates during reduced oxygen conditions is also exhibited by members of the plant kingdom. Mitochondrial respiration within plants is inhibited during hypoxia, meaning that the production of ATP, and subsequently the capacity for energy generation, is reduced (Mustroph et al. 2014). It has been found that many plants have adapted to this reduction in ATP by increasing the production of enzymes that utilise alternative substrates for energy production, one of these substrates being inorganic pyrophosphate (Mustroph et al. 2014). Pyrophosphate is used within a variety of pathways for the production of energy within plants, however one pathway is currently known to be particularly important under hypoxia: the cleavage of sucrose via sucrose synthase (Mustroph et al. 2014). The cleavage of sucrose produces glucose and fructose, which then must be 'activated' by phosphorylation (the addition of a phosphate group). This entire process usually involves 2 mole of ATP, however the enzyme sucrose synthase can instead utilise 1 mole of pyrophosphate to produce the same net energy output for half the energy input (Mustroph et al. 2014). This reduction in energy input allows the organism to conserve ATP, which is useful under hypoxia as the net production of ATP will be reduced due to the cessation of aerobic respiration. Sucrose synthase has been identified in many plant varieties, and its induction under low oxygen conditions has been observed in groups such as rice, cotton, soybean and poplar (Mustroph et al. 2014 and therein). Additionally, the activity and/or protein content of sucrose synthase is increased under low oxygen conditions in potatoes, wheat and rice (Mustroph et al. 2014 and therein). This all points to evidence of increased utilisation of inorganic pyrophosphate during hypoxia, and furthermore the importance of anaerobic metabolic pathways and alternative energy substrates during low oxygen conditions.

A.6 — Insect respiratory system regulation

Many insects regulate the levels of carbon dioxide (CO_2) and O_2 within their respiratory systems using a discontinuous gas-exchange cycle (DGC, Lighton 1996). This cycle consists of multiple phases: initially the spiracles are closed, and the insect utilises O_2 stored within its respiratory system for respiration (the C phase). Whilst O_2 is consumed, CO_2 builds up within the insect, thus decreasing the endotracheal pressure of O_2 within the insect. After a critical concentration of O_2 is reached (~5kPa, ~23.8% PAL), the muscles maintaining the closure of the spiracles are periodically inactivated, causing the spiracles to 'flutter' open and closed (F phase). This causes O_2 to diffuse into the tracheal system, supplying the insect with sufficient O_2 for aerobic tissue respiration (Lighton 1996). Multiple authors have suggested different reasons as to why the DGC initially arose, with some claiming it was an adaptation to the hypoxic conditions of underground burrows (Lighton 1998), and others theorising the discontinuous breathing method is used to avoid oxygen toxicity (Hetz & Bradley 2005). No matter the original reason for the evolution of the DGC, it is clear that it is an effective system for the control of gas exchange, and therefore is a valuable tool in the insect hypoxic response. Insects using DGC are shown to exhibit consistent responses when exposed to decreased ambient O_2: the C phase becomes shorter, and the rate of CO_2 emission increases during the F phase (Harrison et al. 2006), which both allow for O_2 diffusion to increase in speed. It should also be noted, however, that the effects of ambient O_2 on the DGC depend somewhat on the insect species: the duration of the cycle can be increased, decreased, or unaffected as a result of ambient O_2 fluctuations (Harrison et al. 2006).

The DGC is not the only physiological alteration that the insect respiratory system utilises in response to hypoxia. Insects have also been known to alter their spiracles in multiple ways when exposed to hypoxia, causing them to open more frequently, wider, or for longer durations (Wigglesworth 1935; Case 1956; Harrison et al. 2006), allowing for the maintenance of O_2 diffusion within their tissues even at lower oxygen concentrations. Additionally, it is possible for insects to compress regions of their body to create convective gas flow – these movements are stimulated by hypoxia, and suppressed by hyperoxia (Harrison et al. 2006).

A.7 — Extent of hypoxic environments on Earth, and the biomass within these environments

The definition of hypoxia in aquatic settings is different to that of atmospheric/cellular hypoxia, due to the differences in the diffusion of gases in water compared to air: the diffusion coefficient for O_2 in air is ~8000-times greater than that for water (Dejours 1989). Aquatic hypoxia is therefore most commonly cited as being <0.2 ml O_2/L of

water (Kamykowski & Zentara 1990), with OMZs containing <0.5 ml O_2/L (Levin 2003). Helly & Levin (2004) used both of these thresholds to determine the approximate extent of global aquatic hypoxia in the early 2000s, finding that ~1 000 000 km^2 of ocean floor was overlain with water containing <0.5 ml O_2/L, and 764 000 km^2 of ocean floor was overlain with water <0.2 ml O_2/L. This area has likely increased since this time, due primarily to anthropogenic activity increasing eutrophication and atmosphere-ocean cycling (Diaz & Rosenberg 2008). Despite the low oxygen conditions of OMZs, life is still abundant within these environments. For example, Levin (2003) collated data on the density of various groups of organisms within OMZs worldwide, finding foraminifera to be especially abundant within OMZs, with densities as high as ~16 000 individuals/10 cm^{-3} off the coast of Oman (Gooday et al. 2000). Foraminifera are far from the only organisms identified within OMZs however, with benthic metazoan meiofauna seemingly reaching their maximum densities at the lowest oxygen concentrations within OMZs, and nematode densities possibly being up to 5-times higher within OMZs than underneath them (Levin 2003). Levin also noted that nematodes appear to make up ~95% of benthic metazoan meiofauna at low oxygen concentrations. Benthic macrofauna (~300–500 μm) are often less abundant in OMZs, with their densities being especially depressed in the 'core' of OMZs where concentrations are ~0.15 ml O_2/L (Levin 2003). Despite this, Levin still reported a macrofaunal density of ~21 000 individuals/m^{-2} on the central Chile margin (0.13 ml O_2/L), indicating that larger life can also still be abundant at lower O_2 concentrations. Benthic megafauna (e.g., crustaceans, echinoderms) are admittedly nearly absent from OMZ cores in general (Levin 2003), however they can be found in surprisingly high abundances near the lower boundaries of OMZs, as well as in the cores of some OMZs with slightly higher O_2 concentrations (e.g., hermit crabs off central California, with 0.27 ml O_2/L, Thompson et al. 1985; Levin 2003). The high density of fauna, up to and including benthic megafauna, within OMZs worldwide is one line of evidence for the global hypoxic niche being continuously inhabited, possibly indicating a role for hypoxia in the life cycle of many multicellular organisms.

The subsurface of Earth is also a heavily populated environment. Defined in Whitman et al. (1998, pg. 1) as being "terrestrial habitats below 8 m and marine sediments below 10 cm", the extent of this low-oxygen environment is difficult to determine, due largely to the general inaccessibility of it. However many authors have attempted to estimate the subsurface biomass. Whitman et al. (1998) estimated prokaryotic abundance in a number of environments on Earth, concluding that soils contained ~2.56 x 10^{29} prokaryotic cells, and unconsolidated subsurface marine sediments contained ~3.8 x 10^{30} prokaryotic cells. The total global prokaryotic abundance and biomass, for comparison, was estimated at 4.15–6.4 x 10^{30} cells, or 353–546 Pg carbon (C) (1 Pg = 10^{15} g) (Whitman et al. 1998). This estimate later came under scrutiny, particularly by Kallmeyer et al. (2012), who estimated the prokaryotic cell abundance of subseafloor sediment to be ~2.9 x 10^{29} cells (4.1 Pg C), 50–78% less than the estimate of Whitman et al. (1998). Despite this, subsequent estimates utilising new data concluded that the evidence still supported the results of Whitman et al. (1998), with 10^{16}–10^{17} g C estimated for the deep continental biomass (McMahon & Parnell 2014). One of the most recent estimates of subsurface biomass comes from Bar-On et al. (2018), who estimated a microbial soil and deep subsurface biomass of ~100 Gt C (1 Gt = 1 Pg), with the estimate for total global biomass being ~550 Gt C. Additionally, it has been suggested that the deep biosphere comprised a carbon reservoir 1–15-times as large as that of the surface biosphere during the period 2.0–0.4 Ga (McMahon & Parnell 2018).

The deep subsurface biosphere is subject to a number of life-limiting factors that are not present in most environments on the surface of the Earth, such as extremes of temperature and pressure, as well as very low O_2 concentrations (Kieft 2016). It is therefore difficult to accurately assess the areal extent of the deep subsurface biosphere (i.e. the area within which life can survive in the deep subsurface is limited in large part by these extreme conditions). According to models, the abundance and density of life decreases with depth in the subsurface biosphere (McMahon & Parnell 2014), and the current known upper temperature limit of life is ~122°C (Takai et al. 2008). Combining this apparent upper limit with data for average geothermal gradients, Kieft (2016) estimated the limit of life could be 2–12 km below the land surface. This author also notes that for regions with lower geothermal gradients, the biosphere may extend greater than twice as deep as has been currently probed, exceeding ~10 km depth (e.g., in the Witwatersand Basin, with a geothermal gradient of 8–10°C km^{-1}, Kieft 2016). Regardless of how deep the subsurface biosphere extends, it is clear that low-oxygen environments make up a large portion of the known habitable niches on Earth, and the organisms within them form a large part of the global biomass.

When thinking about the deep subsurface, it is natural to assume that the life here is simple and unicellular, and indeed the majority of life within the deep biosphere is prokaryotic (Bar-On et al. 2018). However, there is also evidence of more complex, multicellular life within these environments. Fungi, for example, are reported to have an essential role in important biogeochemical cycles in the deep biosphere, being widespread up to 1 km deep in the continental crust (Drake & Ivarsson 2018). Interestingly, whilst this environment is anoxic, the majority of fungi in

the subsurface are species which are known aerobes in surface environments (Drake & Ivarsson 2018), suggesting that very low oxygen concentrations do not limit the functions of many species of fungi. This also introduces the possibility that fungi are capable of switching between aerobiosis and anaerobiosis depending on the ambient oxygen conditions. It has also been suggested that the ecological role of fungi in OMZs has been underestimated (Jebaraj et al. 2010), indicating that fungi are abundant and important in a wide variety of hypoxic habitats. It should be noted here that these fungi were performing anaerobic processes, and thus utilising alternative nutrients than oxygen. The alternative nutrients utilised by these fungi in the absence of oxygen are not currently known (Drake & Ivarsson 2018), however many fungi are known to utilise nitrate (NO_3^-) and nitrite (NO_2^-) under anaerobic conditions. The availability of nitrate and nitrite ions for anaerobic processes relies somewhat on the previous presence of oxygen. In turn this would suggest that the success of this type of anaerobic metabolism in the deep subsurface of a planet would require that the planet had been somewhat oxygenated at some point in time, and therefore that perhaps higher levels of atmospheric oxygen are required even for the initial development of the substrates of anaerobic metabolism. However, it is still possible that these fungi were utilising substrates devoid of oxygen for their anaerobic metabolism, and this is still evidence that fungi form essential parts of biogeochemical cycles within low-oxygen environments.

The most exciting form of large life to be identified in the deep subsurface thus far are nematodes discovered in groundwater at depths of 0.9–3.7 km (Borgonie et al. 2011). This discovery compliments a growing body of evidence that proves it is possible for complex multicellular life (including metazoans) to survive in hypoxic/anoxic conditions. Danovaro et al. (2010), for example, identified three new Loriciferan species living in permanently anoxic conditions within the sediments of the L'Atalante basin in the Mediterranean Sea. This discovery was very important for the study of the metazoan relationship with oxygen as these individuals were found to operate through obligate anaerobiosis, presumably suggesting they are intolerant to PAL of O_2. These species were found to not possess mitochondria (the energy-producing organelle of choice for most aerobic eukaryotes), but instead they possess hydrogenosomes, which are known to be utilised by anaerobic organisms to produce energy through the reduction of pyruvate rather than oxygen (Lindmark & Müller 1973). This obligate anaerobiosis was previously only observed in unicellular eukaryotes (Danovaro et al. 2010). The authors concluded that this metabolic pathway was an adaptation to the anoxic conditions in which the individuals lived, however under the assumption that hypoxia is required for multicellular life, perhaps the reverse is true – these species simply 'retained' the traits which were once exhibited by all early metazoans before the group expanded into the oxic world.

In addition to the hypoxic environments discussed above, other low-oxygen environments of course exist on Earth. Therefore the total low-oxygen niche on Earth, and the total biomass within these environments, are both likely much greater than estimated. One such environment is sulphidic cave systems, populated predominantly by chemolithoautotrophic microorganisms (Engel 2007). The global biomass of these caves is difficult to determine, considering that: the full global extent of sulphidic cave systems is not currently known; they are difficult to physically study; and most of the organisms within these environments are microscopic. Despite this, some authors theorise that the primary productivity of chemolithotrophs may surpass the primary productivity exhibited by photosynthetic organisms on the surface of the Earth (Stevens 1997). This is another example of just how influential low-oxygen environments are for Earth's biosphere, as well as expanding the extent of the known hypoxic niche.

Appendix B – Experiment methods/results

B.1 — Expansion of the hypoxic niche results

B.1.1 — Fine sediment, unclaved, 21% oxygen

The profile taken within this sample on day 1 was almost identical to that of day 2, so is not included in the corresponding graph (fig. 3A). On days 1 and 2, this sample shows very little variation throughout the whole profile, with only a slight decrease to ~260 μmol/L at the bottom of the profile from a starting position of ~275 μmol/L. On day 3, the water oxygen concentration is slightly lower, remaining at ~265 μmol/L until the sediment-water interface, at which point the concentration begins to decrease until it reaches ~180 μmol/L at ~26 mm profile depth (~15 mm sediment depth). The profile then increases at a much slower pace than the previous decrease until it reaches the end of the profile, at a final concentration of ~220 μmol/L. On day 4 the water oxygen concentration begins at ~225 μmol/L, and is relatively stable before a slight increase beginning at ~7 mm profile depth (~4 mm above the sediment-water interface) to ~235 μmol/L. This is then followed by a rapid decrease when crossing the sediment-water interface, with the concentration reaching 0 μmol/L by ~20 mm profile depth (~9 mm sediment depth). The vertical extent of the hypoxic zone within this profile is ~4.5 mm; the previous profiles did not reach hypoxia.

B.1.2 — Coarse sediment, unclaved, 21% oxygen

As can be seen in fig. 3B, on day 2 the water oxygen concentration began ~275 µmol/L, where it remained until ~17 mm profile depth, at which point the concentration began to decrease very slowly, dropping by a total of ~10 µmol/L by the sediment-water interface. This decrease pattern continued at roughly the same pace for the remainder of the profile, eventually reaching ~235 µmol/L. On day 3, the water oxygen concentration was very stable, remaining at ~240 µmol/L until the sediment-water interface. When entering the sediment the concentration decreased more rapidly than on day 2, however the decrease was still relatively small, reaching ~190 µmol/L at ~35 mm profile depth (~12 mm sediment depth) before becoming more stable once again. The concentration remained within this range of 190 ± 10 µmol/L for the remainder of the profile. The profile on day 4 follows a very similar pattern to that of day 3, with the concentration remaining at ~270 µmol/L throughout the water column, and decreasing at a similar rate to that of day 3 when entering the sediment. At ~35 mm profile depth (the depth at which the day 3 profile stopped decreasing as rapidly), the day 4 profile reached ~185 µmol/L, and also stopped decreasing so rapidly. The day 4 profile then remained at 185 ± 5 µmol/L for the remainder of the profile. None of the profiles taken within this sample reached hypoxia.

B.1.3 — Fine sediment, autoclaved, 21% oxygen

As seen from fig. 3C, the oxygen concentration on day 1 remained stable at ~245 µmol/L throughout the water column, decreasing very slightly to ~240 µmol/L by the sediment-water interface. After entering the sediment, the profile continues to decrease slightly until ~41 mm profile depth (~22 mm sediment depth), where it reaches ~210 µmol/L and begins to increase very slowly to reach ~220 µmol/L by the end of the profile. On day 2, profile 1 begins at roughly the same water concentration as day 1, remaining ~240 ± 5 µmol/L throughout the water column. When entering the sediment, this profile decreases much faster than day 1, reaching ~110 µmol/L by ~34 mm profile depth (~15 mm sediment depth), before increasing again to ~180 µmol/L by the end of the profile. Profile 2 of day 2 has a lower water oxygen concentration than the previous profiles (~210 µmol/L), and remains within ~10 µmol/L throughout the water column. Within the sediment, the profile decreases to reach ~20 µmol/L by ~32 mm profile depth (~13 mm sediment depth), before increasing more rapidly to ~140 µmol/L by the end of the profile. The day 3 profile begins at a lower concentration than all the other profiles, remaining ~170 µmol/L throughout the water column and the first 1 mm of sediment, before decreasing rapidly to reach 0 µmol/L by ~26 mm profile depth (~7 mm sediment depth). The hypoxic zone has a vertical extent of ~22 mm on day 2 (profile 2 only), decreasing quickly to ~4.25 mm by day 3.

B.1.4 — Fine sediment, double-autoclaved, 10% oxygen

The 21% oxygen 'control' profile taken on the day after sample creation (day 2) began with an oxygen concentration of ~225 µmol/L in the water overlying the sample, decreasing slowly until a concentration of ~200 µmol/L was reached at the sediment-water interface at roughly 14 mm profile depth (fig. 4A). After entering the sediment, the oxygen concentration continued to decrease at a slightly faster pace, reaching ~130 µmol/L by 30 mm profile depth, at which point the decrease slowed once more, reaching ~90 µmol/L by the end of the profile at 70 mm depth.

After the O_2 concentration was reduced and the sample was covered with Parafilm for ~3 hours, the 10% oxygen profile also taken on day 2 began with a water oxygen concentration of ~180 µmol/L and remained relatively stable throughout the water column, decreasing by ~20 µmol/L before reaching the sediment-water interface. Within the sediment, there was a rapid decrease of oxygen concentration, falling to ~60 µmol/L at 6 mm sediment depth, followed by a slightly slower decrease to 0 µmol/L by ~30 mm of profile depth (16 mm sediment depth). After maintaining the water oxygen concentration through bubbling with 10% O_2, the profiles from day 3 and day 4 follow a very similar pattern: both profiles reach 0 µmol/L by ~30 mm profile depth, as well as very similar water oxygen concentrations, apart from some slight variations.

The day 5 profile was taken first thing in the morning after the sample was left covered overnight, and begins with a much higher water oxygen concentration of ~225 µmol/L, displaying very little variation from this value until reaching the sediment-water interface. After entering the sediment, the concentration decreases very rapidly to 0 µmol/L (within ~7 mm of sediment depth), and remains at this value for the entire profile. The day 9 profile was taken after leaving the sample to rest covered for two days, then reducing the water concentration with dithionite and leaving to rest for ~1.5 hours. The water oxygen concentration was stable at ~125 µmol/L for ~5 mm, before increasing rapidly to ~180 µmol/L, and decreasing back to 125 µmol/L at the sediment-water interface. Within the first millimetre of sediment, there was a slight increase of oxygen concentration by ~15 µmol/L before a rapid decrease to 0 µmol/L at 22.5 mm profile depth (8.5 mm sediment depth). This profile also closely follows the

pattern of days 2, 3 and 4, with a major difference being the more 'curved' appearance of the decrease patterns of the previous profiles, whilst the day 9 profile has a decrease which is more 'flat'.

The vertical extent of the hypoxic zones on days 2 and 3 are fairly similar at 10–10.5 mm. This increases slightly on day 4 to ~12.5 mm, before decreasing significantly by day 5 to ~5.25 mm. The vertical extent is still at a similar value by day 9, at ~5.75 mm.

B.1.5 — Coarse sediment, double-autoclaved, 10% oxygen

The 21% oxygen control profile taken on day 2 follows a very similar pattern to that of the fine double-autoclaved sediment, with a slightly lower concentration: the profile begins at ~225 μmol/L at the top of the water column, followed by a slow decrease to ~185 μmol/L by the sediment-water interface (fig. 4B). After entering the sediment, the decrease appears to continue at the same pace until ~17 mm into the sediment, at which point the concentration is ~135 μmol/L, and the profile levels out. The decrease continues at a slower pace until the end of the profile, at which point there is a brief, sharp negative excursion and the profile reaches ~100 μmol/L.

The 10% oxygen profile taken on day 2 begins at a water concentration of ~135 μmol/L, where it remains until ~10 mm of profile depth, at which point the concentration begins to decrease before reaching ~90 μmol/L at the sediment-water interface. Within the sediment the decrease continues at a slightly slower pace until ~20 mm of profile depth (~7 mm of sediment depth), where the profile reads ~10 μmol/L before continuing to decrease much more slowly to reach 0 μmol/L by ~25 mm of profile depth (~12 mm sediment depth).

The day 3 profile begins at a water oxygen concentration of ~180 μmol/L, and remains within ±10 μmol/L of this value throughout the water column. The concentration begins to decrease rapidly slightly above the sediment -water interface, decreasing to ~30 μmol/L by ~21.5 mm profile depth (~8.5 mm sediment depth). This is followed by a much slower decrease to 0 μmol/L by ~27 mm of profile depth, slightly deeper than the previous day. The day 4 profile follows a very similar pattern, especially within the sediment, although this profile shows a much smoother decrease than day 3. The water oxygen concentration of day 4 begins ~160 μmol/L, and initially shows a slight increase to ~170 μmol/L, before beginning to decrease at the same depth as day 3, slightly above the sediment-water interface. Both profiles reach 0 μmol/L at roughly the same sediment depth.

The day 5 profile begins ~190 μmol/L in the water column, and slowly increases to ~200 μmol/L by the sediment-water interface. It then shows a similarly rapid decrease to the previous days, albeit with a higher overall concentration. The concentration drops to ~30 μmol/L by ~24 mm profile depth (~11 mm sediment depth), before decreasing more slowly to reach 0 μmol/L by ~32.5 mm profile depth (~19.5 mm sediment depth). Similarly to the previous profiles, this profile reaches 0 μmol/L at a greater depth.

The profiles of days 8 and 9 have fairly similar patterns, especially when it comes to the water oxygen concentrations: both profiles remain ~170 μmol/L throughout the entire water column. When entering the sediment, both profiles also initially display very similar patterns of decrease, down to a profile depth of ~21 mm (~8 mm sediment depth), by which point the oxygen concentration has decreased to ~90 μmol/L. After this point, the profiles diverge slightly more: the day 8 profile decreases slightly less rapidly than day 9, eventually reaching 0 μmol/L by ~41 mm profile depth (~28 mm sediment depth); the day 9 profile initially decreases more rapidly, reaching ~30 μmol/L by ~16 mm sediment depth. After this, the profile decreases more slowly to reach 0 μmol/L at roughly the same level as the profile of day 8. Both of these profiles reach 0 μmol/L much deeper than the profiles of the previous days.

The vertical extent of the hypoxic zone is fairly similar from days 2–5, being ~10 mm on day 2, ~9 mm for days 3 and 4 and increasing slightly to ~10.5 mm on day 5. By day 8, the vertical extent has increased greatly to ~17 mm, increasing slightly again to reach ~17.5 mm on day 9.

B.2 — Exoplanet oxygen fugacity method

Step 1: Calculate the ratio of the abundance of each metal compared to the abundance of oxygen, Z/O, using Equations 1 and 2:

Eq. 1: $$\log(Z/O) = \log(Z/X) - \log(O/X)$$

Eq. 2: $$Z/O = 10^{\log(Z/O)}$$

Where Z = the atomic abundance of the metal (Si, Mg, Al, Ca or Fe), X = atomic abundance of H or He (this depends on the type of white dwarf), and O = atomic abundance of oxygen. The values used for this step are available in table 1.

Step 2: Assign O atoms to Si, Mg, Al and Ca to form metal oxides using the relationships between Z/O and the number of O atoms required by each oxide, (O)i, below:

$$(O)SiO_2 = 2*Si/O$$

$$(O)MgO = Mg/O$$

$$(O)Al_2O_3 = (3/2)*Al/O$$

$$(O)CaO = Ca/O$$

It is important to note here that from this point forward, total oxygen, O_{total}, does not have the same value as atoms of oxygen assigned to each oxide, (O)i.

Step 3: Next, calculate the excess oxygen available for bonding with Fe (O_{XS}) relative to O_{total} using Equation 3:

Eq. 3: $$O_{XS} = 1 - (O)SiO_2 - (O)MgO - (O)Al_2O_3 - (O)CaO$$

O_{XS} is then assigned to Fe to create FeO (representing all possible oxides of iron present within the WD atmosphere). The value of FeO for use in the following calculations is dependent on the relationship between O_{XS} and Fe/O (calculated in Step 1):

$$\text{If } Fe/O > O_{XS}, \text{ then } FeO = O_{XS}$$

$$\text{If } Fe/O < O_{XS}, \text{ then } FeO = Fe/O$$

Step 4: Calculate the mole fraction of FeO for the material accreted to the white dwarf in question (*x*FeO), using the ratios of all the metal oxides relative to O_{total}, as well as that for FeO calculated above. The oxide ratios for the remaining metals can be calculated using the relationships below:

$$SiO_2 = Si/O$$

$$MgO = Mg/O$$

$$Al_2O_3 = 0.5*Al/O$$

$$CaO = Ca/O$$

*x*FeO is then calculated using Equation 4:

Eq. 4: $$xFeO = \frac{FeO}{FeO + SiO2 + MgO + Al2O3 + CaO}$$

Step 5: Calculate the oxygen fugacity for the polluted WD relative to the iron-wüstite standard (ΔIW) using the *x*FeO calculated above with Equation 5:

Eq. 5: $$\Delta IW = 2 \log * \left(\frac{xFeO}{0.85}\right)$$

Where 0.85 is the nominal mole fraction of Fe in the metal phase during the formation of the parent body which

polluted the WD.

In order to determine the uncertainties (plus and minus errors) associated with the calculated fO_2 values for each polluted WD, the uncertainties with each step must be calculated according to the method below:

Step 6: To calculate the uncertainties of the log(Z/O) values (σlog(Z/O)) use Equation 6:

Eq. 6:
$$\sigma\log(Z/O) = \sqrt{\sigma^2\log(Z/X) + \sigma^2\log(O/X)}$$

Where σlog(Z/X) is the error associated with the abundance of each metal ion that is polluting the WD atmosphere and σlog(O/X) is the error associated with the abundance of oxygen in the WD atmosphere (see table 1 for these errors).

Step 7: To calculate the uncertainties associated with the Z/O values, σZ/O, use Equation 7:

Eq. 7:
$$\sigma Z/O = Z/O * \ln(10) * \sigma\log(Z/X)$$

Where Z/O represents the metal abundances compared to oxygen, calculated using Equation 2 during Step 1.

Step 8: Next, the uncertainty in excess oxygen, σO_{XS}, can be calculated using Equation 8:

Eq. 8:
$$\sigma O_{XS} = \sqrt{4 * \sigma^2 Si/O + \sigma^2 Mg/O + (3/2)^2 * \sigma^2 Al/O + \sigma^2 Ca/O}$$

In a similar way that O_{XS} was assigned to Fe above, σO_{XS} can be used to determine the uncertainty in FeO/O (σFeO):

$$\text{If } O_{XS} > Fe/O, \text{ then } \sigma FeO = \sigma Fe/O$$

$$\text{If } O_{XS} < Fe/O, \text{ then } \sigma FeO = \sigma Oxs$$

Step 9: The uncertainty in mole fraction of Fe, σ*x*FeO, can then be calculated using Equation 9:

Eq. 9:
$$\sigma xFeO = \sqrt{\left(\frac{(\sum i - FeO)}{\sum i^2}\right) * \sigma^2 FeO + \left(\frac{-FeO}{\sum i^2}\right)^2 * \sigma^2 SiO_2 + \left(\frac{-MgO}{\sum i^2}\right)^2 * \sigma^2 MgO + \left(\frac{-Al_2O_3}{\sum i^2}\right)^2 * \sigma^2 Al_2O_3 + \left(\frac{-CaO}{\sum i^2}\right)^2 * \sigma^2 CaO}$$

Where ∑i represents the sum of all metal oxides (SiO_2, MgO, Al_2O_3, CaO and FeO) that were calculated previously.

Step 10: Finally, to calculate the plus and minus error of each ΔIW value, use Equations 10–13:

Eq. 10:
$$\Delta IWmin = 2 * \log 10 * \left(\frac{(FeO - \sigma FeO)}{0.85}\right)$$

Eq. 11:
$$\Delta IWmax = 2 * \log 10 * \left(\frac{(FeO + \sigma FeO)}{0.85}\right)$$

Eq. 12:
$$\text{Plus error} = \Delta IWmax - \Delta IW$$

Eq. 13:
$$\text{Minus error} = \Delta IW - \Delta IWmin$$

B.3 — Exoplanet oxygen fugacity results

B.3.1 — *Doyle et al. 2019*

B.3.1.1 — He-dominated

WD 1145+017 has a temperature of 16 900 K, with an fO_2 of ΔIW -0.568. The positive error for this fO_2 is +0.118, and the negative error is -0.136. WD 1536+520 (20 800 K) has a much lower oxygen fugacity of -1.34, and also has much larger positive and negative errors of +0.387 and -0.717 respectively. GD 40 has a much lower temperature (15 300 K) but a relatively similar fO_2 of -1.14. The errors for this value are +0.292 and -0.443. The final He-dominated WD from this study, J0738+1835, has an even lower temperature of 13 950 K, but again a fairly similar fO_2 (-1.12), and positive and negative errors of +0.188 and -0.240 respectively.

B.3.1.2 — H-dominated

There are only two H-dominated WDs present within this study, with the data sourced from Doyle et al. (2019b). The papers from which the original data was sourced for these WDs (i.e. the data which Doyle et al. (2019a) corrected for settling times) are Gänsicke et al. (2012) and Melis & Dufour (2017). WD 1226+110 has a temperature of 20 900 K and an fO_2 of -0.536 (positive error +0.288, negative error -0.435). J1043+0855 has a slightly lower temperature of 18 330 K, but a substantially lower fO_2 of -1.84 with a positive error of +0.658 (negative error was not able to be calculated for this WD).

B.3.2 — *Harrison et al. 2018*

GD 362 has a temperature of 10 500 K and an fO_2 of ΔIW -0.665. The positive and negative errors associated with this value are +0.188 and -0.241 respectively. PG 1225-079 has a similar temperature at 10 800 K, accompanied by a slightly lower fO_2 of -0.865. The errors for this value are also slightly smaller than those of GD 362, with +0.132 and -0.155 positive and negative errors respectively. J1242+5226 has a significantly lower fO_2 of -1.833, despite having a relatively higher temperature of 13 000 K. The errors are similarly large, with a positive error of +0.485 and negative error of -1.196. HS 2253+8023 is not much hotter than the previous WD at 14 400 K, but has an increasingly positive fO_2 value (-0.887), as well as the smallest errors within this study (+0.054 and -0.057 respectively). G241-6 is 15 300 K and has an fO_2 of ΔIW -1.5. The errors for this value are rather large, with a positive error of +0.378 and negative error of -0.685. GD 61 (17 300 K) and J0845+2257 (19 780 K) have the most negative fO_2 values discussed so far, with -2.62 and -3.685 respectively. GD 61 has a positive error of +1.153, and J0845+2257 has the largest positive error of the study with +2.848. No negative errors could be calculated for these WDs.

B.3.3 — *Doyle 2021*

GALEX J2339 has a temperature of 13 735 K and an fO_2 of -1.454, with positive and negative errors of +0.386 and -0.711 respectively. GD 378 has a slightly higher temperature of 15 620 K, accompanied by a more positive fO_2 of -0.974. The associated errors for this WD are +0.344 and -0.579. WD 0446-255 (10 120 K) has a very similar fO_2 to GALEX J2339, with ΔIW -1.418. The positive and negative errors for this WD are slightly lower than for GALEX however, with +0.203 and -0.265 respectively. WD 1232+563 is 11 787 K, and has an fO_2 of -1.189, with errors of +0.194 and -0.251. Finally, WD 2207+121 and WD 1551+175 have essentially identical temperatures (14 752 K and 14 756 K respectively), but relatively different fO_2 values of -1.295 and -1.351 respectively. Their associated errors also differ: WD 2207+121 has a positive error of +0.240 and negative error of -0.333, whilst WD 1551+175 has a positive value of +0.174 and a negative value of -0.218.

Tidigare skrifter i serien ”Examensarbeten i Geologi vid Lunds universitet”:

577. Wahlquist, Per, 2019: Undersökning av mindre förkastningar för vattenuttag i sedimentärt berg kring Kingelstad och Tjutebro. (15 hp)
578. Gaitan Valencia, Camilo Esteban, 2019: Unravelling the timing and distribution of Paleoproterozoic dyke swarms in the eastern Kaapvaal Craton, South Africa. (45 hp)
579. Eggert, David, 2019: Using Very-Low-Frequency Electromagnetics (VLF-EM) for geophysical exploration at the Albertine Graben, Uganda - A new CAD approach for 3D data blending. (45 hp)
580. Plan, Anders, 2020: Resolving temporal links between the Högberget granite and the Wigström tungsten skarn deposit in Bergslagen (Sweden) using trace elements and U-Pb LA-ICPMS on complex zircons. (45 hp)
581. Pilser, Hannes, 2020: A geophysical survey in the Chocaya Basin in the central Valley of Cochabamba, Bolivia, using ERT and TEM. (45 hp)
582. Leopardi, Dino, 2020: Temporal and genetical constraints of the Cu-Co Vena-Dampetorp deposit, Bergslagen, Sweden. (45 hp)
583. Lagerstam Lorien, Clarence, 2020: Neck mobility versus mode of locomotion – in what way did neck length affect swimming performance among Mesozoic plesiosaurs (Reptilia, Sauropterygia)? (45 hp)
584. Davies, James, 2020: Geochronology of gneisses adjacent to the Mylonite Zone in southwestern Sweden: evidence of a tectonic window? (45 hp)
585. Foyn, Alex, 2020: Foreland evolution of Blåisen, Norway, over the course of an ablation season. (45 hp)
586. van Wees, Roos, 2020: Combining luminescence dating and sedimentary analysis to derive the landscape dynamics of the Velická Valley in the High Tatra Mountains, Slovakia. (45 hp)
587. Rettig, Lukas, 2020: Implications of a rapidly thinning ice-margin for annual moraine formation at Gornergletscher, Switzerland. (45 hp)
588. Bejarano Arias, Ingrid, 2020: Determination of depositional environment and luminescence dating of Pleistocene deposits in the Biely Váh valley, southern foothills of the Tatra Mountains, Slovakia. (45 hp)
589. Olla, Daniel, 2020: Petrografisk beskrivning av Prekambriska ortognejser i den undre delen av Särvskollan, mellersta delen av Skollenheten, Kaledonska orogenen. (15 hp)
590. Friberg, Nils, 2020: Är den sydatlantiska magnetiska anomalin ett återkommande fenomen? (15 hp)
591. Brakebusch, Linus, 2020: Klimat och väder i Nordatlanten-regionen under det senaste årtusendet. (15 hp)
592. Boestam, Max, 2020: Stränder med erosion och ackumulation längs kuststräckan Trelleborg - Abbekås under perioden 2007 -2018. (15 hp)
593. Agudelo Motta, Laura Catalina, 2020: Methods for rockfall risk assessment and estimation of runout zones: A case study in Gothenburg, SW Sweden. (45 hp)
594. Johansson, Jonna, 2020: Potentiella nedslagskratrar i Sverige med fokus på Östersjön och östkusten. (15 hp)
595. Haag, Vendela, 2020: Studying magmatic systems through chemical analyses on clinopyroxene - a look into the history of the Teno ankaramites, Tenerife. (45 hp)
596. Kryffin, Isidora, 2020: Kan benceller bevaras över miljontals år? (15 hp)
597. Halvarsson, Ellinor, 2020: Sökande efter nedslagskratrar i Sverige, med fokus på avtryck i berggrunden. (15 hp)
598. Jirdén, Elin, 2020: Kustprocesser i Arktis – med en fallstudie på Prins Karls Forland, Svalbard. (15 hp)
599. Chonewicz, Julia, 2020: The Eemian Baltic Sea hydrography and paleoenvironment based on foraminiferal geochemistry. (45 hp)
600. Paradeisis-Stathis, Savvas, 2020: Holocene lake-level changes in the Siljan Lake District – Towards validation of von Post’s drainage scenario. (45 hp)
601. Johansson, Adam, 2020: Groundwater flow modelling to address hydrogeological response of a contaminated site to remediation measures at Hjortsberga, southern Sweden. (15 hp)
602. Barrett, Aodhan, 2020: Major and trace element geochemical analysis of norites in the Hakefjorden Complex to constrain magma source and magma plumbing systems. (45 hp)
603. Lundqvist, Jennie, 2020: ”Man fyller det med information helt enkelt”: en fenomenografisk studie om studenters upplevelse av geologisk tid. (45 hp)
604. Zachén, Gabriel, 2020: Classification of four mesosiderites and implications for their formation. (45 hp)
605. Viðarsdóttir, Halla Margrét, 2020: Assessing the biodiversity crisis whitin the Triassic-Jurassic boundary interval using redox sensitive trace metals and stable carbon isotope geochemistry. (45 hp)

606. Tan, Brian, 2020: Nordvästra Skånes prekambriska geologiska utveckling. (15 hp)
607. Taxopoulou, Maria Eleni, 2020: Metamorphic micro-textures and mineral assemblages in orthogneisses in NW Skåne – how do they correlate with technical properties? (45 hp)
608. Damber, Maja, 2020: A palaeoecological study of the establishment of beech forest in Söderåsen National Park, southern Sweden. (45 hp)
609. Karastergios, Stylianos, 2020: Characterization of mineral parageneses and metamorphic textures in eclogite- to high-pressure granulite-facies marble at Allmenningen, Roan, western Norway. (45 hp)
610. Lindberg Skutsjö, Love, 2021: Geologiska och hydrogeologiska tolkningar av SkyTEM-data från Vombsänkan, Sjöbo kommun, Skåne. (15 hp)
611. Hertzman, Hanna, 2021: Odensjön - A new varved lake sediment record from southern Sweden. (45 hp)
612. Molin, Emmy, 2021: Rare terrestrial vertebrate remains from the Pliensbachian (Lower Jurassic) Hasle Formation on the Island of Bornholm, Denmark. (45 hp)
613. Höjbert, Karl, 2021: Dendrokronologi - en nyckelmetod för att förstå klimat- och miljöförändringar i Jämtland under holocen. (15 hp)
614. Lundgren Sassner, Lykke, 2021: A Method for Evaluating and Mapping Terrestrial Deposition and Preservation Potential-for Palaeostorm Surge Traces. Remote Mapping of the Coast of Scania, Blekinge and Halland, in Southern Sweden, with a Field Study at Dalköpinge Ängar, Trelleborg. (45 hp)
615. Granbom, Johanna, 2021: En detaljerad undersökning av den mellanordoviciska ”furudalkalkstenen” i Dalarna. (15 hp)
616. Greiff, Johannes, 2021: Oolites from the Arabian platform: Archives for the aftermath of the end-Triassic mass extinction. (45 hp)
617. Ekström, Christian, 2021: Rödfärgade utfällningar i dammanläggningar orsakade av *G. ferruginea* och *L. ochracea* - Problemstatistik och mikrobiella levnadsförutsättningar. (15 hp)
618. Östsjö, Martina, 2021: Geologins betydelse i samhället och ett första steg mot en geopark på Gotland. (15 hp)
619. Westberg, Märta, 2021: The preservation of cells in biomineralized vertebrate tissues of Mesozoic age – examples from a Cretaceous mosasaur (Reptilia, Mosasauridae). (45 hp)
620. Gleisner, Lovisa, 2021: En detaljerad undersökning av kalkstenslager i den mellanordoviciska gullhögenformationen på Billingen i Västergötland. (15 hp)
621. Bonnevier Wallstedt, Ida, 2021: Origin and early evolution of isopods - exploring morphology, ecology and systematics. (15 hp)
622. Selezeneva, Natalia, 2021: Indications for solar storms during the Last Glacial Maximum in the NGRIP ice core. (45 hp)
623. Bakker, Aron, 2021: Geological characterisation of geophysical lineaments as part of the expanded site descriptive model around the planned repository site for high-level nuclear waste, Forsmark, Sweden. (45 hp)
624. Sundberg, Oskar, 2021: Jordlagerföljden i Höjeådalen utifrån nya borrningar. (15 hp)
625. Sartell, Anna, 2021: The igneous complex of Ekmanfjorden, Svalbard: an integrated field, petrological and geochemical study. (45 hp)
626. Juliusson, Oscar, 2021: Implications of ice-bedrock dynamics at Ullstorp, Scania, southern Sweden. (45 hp)
627. Eng, Simon, 2021: Rödslam i svenska kraftdammar - Problematik och potentiella lösningar. (15 hp)
628. Kervall, Hanna, 2021: Feasibility of Enhanced Geothermal Systems in the Precambrian crystalline basement in SW Scania, Sweden. (45 hp)
629. Smith, Thomas, 2022: Assessing the relationship between hypoxia and life on Earth, and implications for the search for habitable exoplanets. (45 hp)

LUNDS UNIVERSITET

Geologiska institutionen
Lunds universitet
Sölvegatan 12, 223 62 Lund